AD-A056 038 AERONAUTICAL RESEARCH LABS MELBOURNE (AUSTRALIA) F/G 20/2
DEVELOPMENT OF MICROSTRUCTURE AND ITS RELATIONSHIP TO THE MECHA--ETC(U)
NOV 77 R B NETHERCOTT, J A RETCHFORD

UNCLASSIFIED ARL/MAT.106 NL

1 OF 1
AD
A056 038

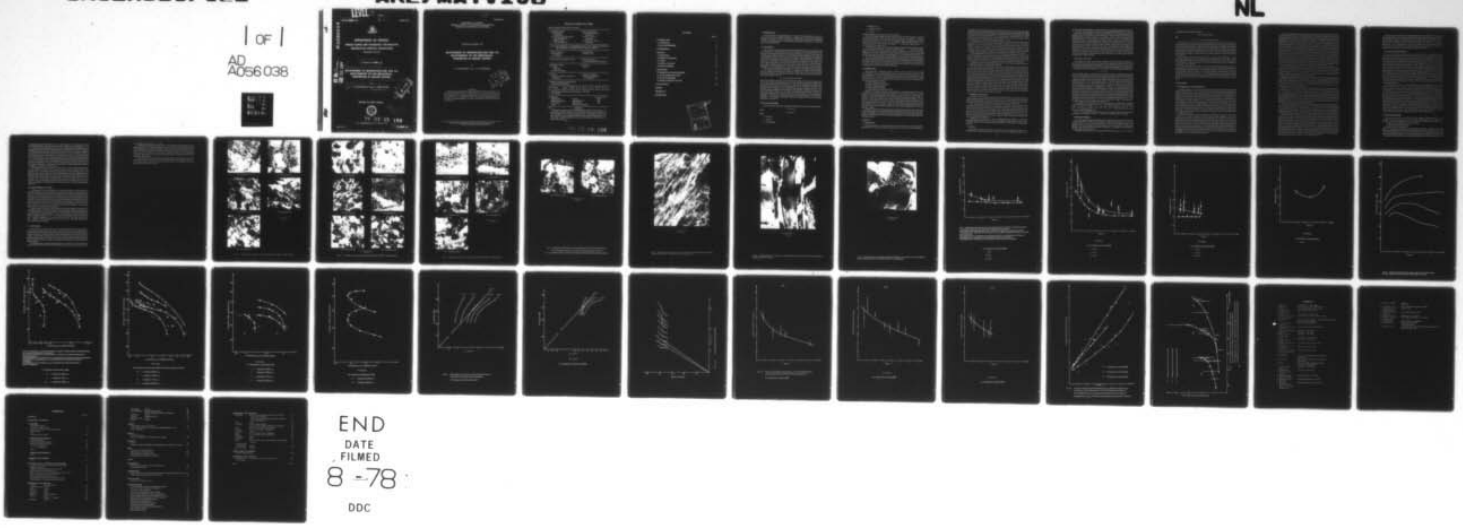

END
DATE
FILMED
8-78
DDC

ARL/Mat-Report-106

AR-000-1102

DEPARTMENT OF DEFENCE

DEFENCE SCIENCE AND TECHNOLOGY ORGANISATION

AERONAUTICAL RESEARCH LABORATORIES

MELBOURNE, VICTORIA

MATERIALS REPORT 106

DEVELOPMENT OF MICROSTRUCTURE AND ITS RELATIONSHIP TO THE MECHANICAL PROPERTIES OF DRAWN COPPER

by

R. B. NETHERCOTT and J. A. RETCHFORD

Approved for Public Release

39 P.

COPY No 8

NOVEMBER 1977

(12)

AR-000-1102

DEPARTMENT OF DEFENCE
DEFENCE SCIENCE AND TECHNOLOGY ORGANISATION
AERONAUTICAL RESEARCH LABORATORIES

MATERIALS REPORT 106

DEVELOPMENT OF MICROSTRUCTURE AND ITS RELATIONSHIP TO THE MECHANICAL PROPERTIES OF DRAWN COPPER

by

R. B. NETHERCOTT and J. A. RETCHFORD

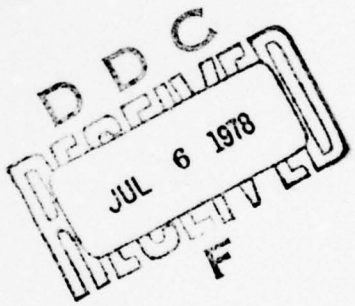

SUMMARY

Dislocation microstructures formed during drawing of copper to strains up to 7, at deformation temperatures between 77 and 473K, have been investigated, together with their relationship to the resulting mechanical properties. The changes in microstructure and tensile flow stress are explained by dynamic recovery and recrystallization processes; correlations of mechanical properties are made with parameters describing the dislocation microstructure.

POSTAL ADDRESS: Chief Superintendent, Aeronautical Research Laboratories,
Box 4331, P.O., Melbourne, Victoria, 3001, Australia.

DOCUMENT CONTROL DATA SHEET

Security classification of this page: Unclassified

1. Document Numbers:
   (a) AR Number:
   AR-000-1102
   (b) Document Series and Number:
   Materials Report 106
   (c) Report Number:
   ARL-Mat-Rept-106

2. Security Classification:
   (a) Complete document:
   Unclassified
   (b) Title in isolation:
   Unclassified
   (c) Summary in isolation:
   Unclassified

3. Title: DEVELOPMENT OF MICROSTRUCTURE AND ITS RELATIONSHIP TO THE MECHANICAL PROPERTIES OF DRAWN COPPER

4. Personal Author(s):
   R. B. Nethercott
   J. A. Retchford

5. Document Date:
   November, 1977

6. Type of Report and Period Covered:

7. Corporate Author(s):
   Aeronautical Research Laboratories

8. Reference Numbers:
   (a) Task:
   DST 76/92
   (b) Sponsoring Agency:

9. Cost Code:
   32 6720

10. Imprint:
    Aeronautical Research Laboratories,
    Melbourne

11. Computer Program(s)—
    (Title(s) and language(s)):
    Not Applicable

12. Release Limitations (of the document):
    Approved for Public Release

12-0. Overseas:	No.		P.R.	1	A		B		C		D		E	

13. Announcement Limitations of the information on this page:
    No Limitation

14. Descriptors:

Microstructure	Drawing	2012
Mechanical Properties	Tensile Properties	2002
Wire Drawing	Deformation	1106
Copper	Dislocations (Materials)	

15. Cosati Codes:

16.

ABSTRACT

Dislocation microstructures formed during drawing of copper to strains up to 7, at deformation temperatures between 77 and 473K, have been investigated, together with their relationship to the resulting mechanical properties. The changes in microstructure and tensile flow stress are explained by dynamic recovery and recrystallization processes; correlations of mechanical properties are made with parameters describing the dislocation microstructure.

CONTENTS

1. INTRODUCTION

The microstructure of metals deformed to low strains (less than about 20%) consists of a fairly uniform network of tangled dislocations. At higher strains, the dislocation arrangement changes to a more open network in which regions of high dislocation density surround regions of much lower dislocation density. This dislocation cell structure is characterisic of a recovered metal in stage III hardening.

1.1 Cell Formation

The reason for cell formation has been treated theoretically by Holt [1], who showed that the driving force for cell formation arises from a reduction in the total elastic energy of the dislocations when they cluster into cell walls. A separate requirement for cell formation is that the dislocations have sufficient mobility out of their slip plane. This requirement is very dependent on the thermal- and stress-activated mobility of dislocations. Holt investigated the stability of a uniformly dense distribution of dislocations with respect to spatial fluctuations in dislocation density. (For convenience, he used an idealised distribution of parallel screw dislocations.) The elastic energy of dislocations in an array consists of two main components: (*a*) their self energy, and (*b*) their interaction energy with other members of the array. The total self energy is independent of the dislocation density if the total number of dislocations remains constant; thus, the only way of reducing the total energy is to reduce the interaction energy component.

It is assumed that the interaction energy for a dislocation is a function of the unmatched positive or negative dislocations in the immediate neighbourhood. This assumption enables the interaction energy to be calculated in terms of a small, cyclic perturbation of dislocation-density ($\Delta\rho$), which has the form

$$\Delta\rho \propto A(\beta).\exp B(\beta).t.\cos(\bar{\beta}\cdot\bar{R})$$

where $A(\beta)$ and $B(\beta)$ are functions of the dislocation distribution, R is the position in the crystal, β is the wave number of the perturbation and t is time. The interaction energy is minimized by growth of the dislocation density fluctuation to a characteristic wavelength. Since $B(\beta)$ occurs exponentially in the equation for $\Delta\rho$, those fluctuations in the dislocation distribution which maximize $B(\beta)$ grow fastest, become dominant, and therefore determine the scale of the dislocation-density modulation. An expression for the perturbation wavelength (λ) that maximizes $B(\beta)$ can be derived in which $\lambda \propto \rho^{-0.5}$ where ρ is the dislocation density and λ is found to be of the same magnitude as the dislocation–dislocation interaction distance. A result of the density modulation is the formation of dislocation cells of size (d) proportional to the fundamental wavelength λ, provided that the dislocation mobility is sufficient to allow the lowest energy configuration to be reached.

1.2 Flow-Stress Relationships

An extension of the expressions introduced in the previous section, using the relationship:

$$\sigma = \alpha.G.b.\rho^{0.5}$$

yields:

$$\sigma \propto G.b.d^{-1.0}$$

where:

σ = flow stress,

α = constant,

G = shear modulus,

b = Burgers vector,

ρ = dislocation density,

d = cell size:

thereby relating flow stress to the size of dislocation cells.

Earlier relationships linking flow stress and grain size have been developed, one of the earliest being ascribed to Hall [2] and Petch [3]. It is of the form $\sigma \propto d^n$ where $n = -\frac{1}{2}$. There is, however, some uncertainty as to the value of the exponent and the conditions under which a conversion from grain size to cell size can be made [4, 5]. When considering flow stress as a function of cell size, several workers [1,6] support $n = -\frac{1}{2}$, whereas in similar metals, $n = -1$ is supported by other workers [7, 8].

A comprehensive study of Cu alloys by Hutchison and Pascoe [9] showed that a range of n values can be measured; however, at the 95% confidence level, $n = -1$ for Cu and its alloys. More recent work, using aluminium [10], indicated a change in the value of the exponent depending on the type of dislocation structure controlling the flow stress and the misfit angle between grains and cells. It appears that an exponent of $-0{\cdot}5$ is appropriate for grains and -1 for cells, with a determining factor being the effective mean free path of a moving dislocation.

The work reported here deals with the formation of the dislocation microstructure during drawing at different temperatures and its effects on the mechanical properties of the resulting wire. The effects of recovery and recrystallization processes on microstructure are also discussed. Changes in tensile flow stresses are explained in terms of these processes and correlations made with parameters describing the dislocation substructure.

2. EXPERIMENTAL

High conductivity (oxygen-free) copper (>99·99%) wires were drawn from annealed 5·7 mm diameter rod to various diameters down to 0·18 mm, i.e. strains (ε) of up to 7. The drawing speed was 8·7 mm/s and the strains per pass were 0·25 plus or minus 0·01 for total strains less than 4·7, 0·16 plus or minus 0·02 for strains from 4·8 to 6·4, and 0·25 plus or minus 0·02 for strains from 6·4 to 7. Colloidal graphite was used as a dry lubricant. The temperatures of drawing were obtained as follows:

(i) Liquid nitrogen bath (77K),
(ii) Dry-ice (CO_2) in alcohol (196K),
(iii) Room temperature (293K),
(iv) Boiling water bath (373K),
(v) Long-nichrome-wound furnace (473K).

Specimens for electron microscopy were obtained by spark machining 0·25 mm thick discs from wires that had been copper electroplated to 3 mm diameter. The discs were then profiled, by jet electropolishing both sides, using 10% nitric acid in water at 293K and at a potential of 150V. The profiled discs were electropolished to perforation using 30% HNO_3 in methanol at 243K and a potential of 6V. The discs were either examined immediately or were stored in a vacuum desiccator to prevent oxidation. Micrographs of sections along the wire axis were obtained using discs cut from wires that had been clamped between glass slides before electroplating; this process produced a copper sheet with the wire running down the centre of the sheet. The discs were examined in transmission, using a Philips EM200 electron microscope operating at 100kV.

Specimens, approximately 60 mm long, were prepared for mechanical testing by painting a 40 mm gauge length with a stopping-off medium before building up each end with electroplated copper, for gripping in pin chucks. Stress-strain characteristics were calculated using load-elongation curves obtained on an Instron tensile testing machine. Constant temperature baths were used where necessary.

3. RESULTS

3.1 Microstructure

Electron microscopy of transverse sections of wires showed that, at strains greater than approximately 0·5, all wires contained dislocation cells. At low strains, the microstructure

consisted of very poorly defined areas of low dislocation density, in a matrix of slightly higher dislocation density. As the strain increased, the low dislocation density areas became more defined and the structure became more clearly cellular, with loose dislocation tangles forming the original cell walls. At a strain of approximately 1·8, for temperatures of drawing from 196 to 373K, the structure consisted of large areas of well-defined cells. These cells were formed by walls of dislocation tangles of higher dislocation density (Figures 1, 2, 3).

At higher strains, the cell walls became more precisely defined and the dislocation tangles reduced in width. The rate at which these changes occurred with strain was a function of temperature, e.g. at 196 and 293K, there were still areas of cells formed by arrays of loose forest tangles at strains of 3·1, whereas at 373K this type of cell system was last observed at a strain of about 1·1. Wires drawn at 473K (Figure 4) contained similar dislocation tangles, but in not such regular arrays as tangles formed at lower temperatures. Nevertheless, the walls, though of a higher dislocation density, still had dislocations trailing out of them into the cell body.

At all temperatures of deformation up to 373K, lamellar deformation twins were also observed, the extent of their occurrence increasing as temperature decreased. At 77K, certain regions contained such a high density of twins (Figure 5) that the dislocation cell structure could not form, whereas at 196K there was a marked decrease in twin occurrence, and at 373K only occasional twins were observed. No deformation twins were observed in 473K specimens.

Longitudinal sections of wires and sheet deformed at 293 and 473K showed that the cells were elongated in the direction of deformation (Figure 6).

At 473K, the microstructure exhibited a general cell structure (Figure 4) somewhat different from that observed at lower temperatures. At all strains investigated (from 0·6 to 6·2), there existed two quite distinct types of boundary. The first was similar to those mentioned previously, and consisted of loose dislocation tangles forming a cell boundary with dislocations trailing into the cell. The second type of boundary was of a much sharper character and appeared to be a higher angle boundary than those for walls composed of dislocation tangles; the walls also had fewer single dislocations trailing from them. This second type of wall is very similar to a grain boundary formed during recrystallization, but on a much smaller scale than usual. The sharp boundaries formed a general grain-type structure inside which dislocation tangles formed smaller cells. Even though the overall structure observed at 473K was not generally found at lower temperatures, there was evidence that the second type of boundary did occur at lower temperatures. For example, at 196K for strains above 3, there were regions in which the second type of narrow boundary was present and bounded cells within which, either very few dislocations were observed, or else cells formed by dislocation tangles occurred (Figure 1(*d*)). At 293 and 373K similar cell structures were found (Figures 2(*e*), 3(*d*)).

3.2 Stability of Microstructure

The stability of the dislocation structure of the deformed state is of particular importance when preparing specimens from deformed material [11, 12]. To investigate the structural stability, specimens were subjected to two types of tests, the first being in-situ heating of foils in the electron microscope, the second being annealing of bulk specimens at various temperatures.

In-situ heating of thin foils of wire, deformed at temperatures between 196 and 473K, showed that the dislocation structure was surprisingly stable until a certain temperature was reached, after which recrystallization rapidly occurred and the dislocation networks were swept away by the advancing new grain boundary. In the copper foils studied, the temperature at which this process occurred was above 800K. Prior to recrystallization, there was very little change in the overall dislocation substructure, thereby indicating that, in foils at least, one can be fairly confident that large-scale dislocation movement, which is a thermally activated process, does not occur after foil preparation.

Annealing bulk specimens for 1 hour at temperatures below 600K also caused little observable change in dislocation cell structure. Above 600K, cell disintegration was seen to occur, although it would seem, by subgrain coalescence [13] (Figure 7) rather than by grain-boundary migration.

3.3 Cell Size

As previously mentioned, the cell size is considered to be an important parameter to be correlated with the mechanical properties of metals, viz. flow stress and hardness. In this work,

the cell sizes have been measured as a function of strain for several temperatures of deformation.

Cell sizes were determined by a mean linear intercept method, using at least 3, and more usually 6, electron micrographs for each strain and temperature. The mean intercepts measured manually were, for the 196, 293 and 373K specimens, compared with those measured using a Quantimet Image Analysing Computer; in most instances, the two results were the same within experimental error. At 373K, however, the manually estimated values were consistently below the Quantimet values by approximately 20%, probably due to a systematic error. The variation of cell sizes with the strain and temperature of deformation (Figure 8) show that, as the strain increases, there is a decrease in cell size, though it appears that the cell size approaches some limiting value and is fairly constant above a strain of 2. The limiting cell sizes for temperatures from 196 to 373K are seen to lie between approximately 0·19 and 0·24 μm. For a deformation temperature of 473K, however, the cell size decreased initially but then increased again after a strain of approximately 3. Another feature to note is that, at any given strain, the cell size does not follow a simple relationship with temperature of deformation, e.g. the cell sizes at 373K lie between those for 196K and 293K.

3.4 Cell Size *v.* Flow Stress

The dislocation cell size has often been correlated with various mechanical properties of metals. In this work, the cell size (d) was compared with the ultimate tensile stress (U.T.S.) of wires measured at the temperature of deformation or lower. The respective values of d and U.T.S. were obtained from the smoothed curves of best fit through the appropriate d *v.* strain and U.T.S. *v.* strain curves, as shown in Figures 8 and 9. The fit that is most often attempted of these data is:

$$\sigma = \sigma_0 + k.d^n$$

where σ_0 is the flow stress of a single crystal or a specimen having a very large cell size (assuming that most of the hardening is governed by the existence of dislocation tangles and cell formation), k and n are constants. Previous work [14] indicates that the flow stress at low strains, for recrystallized copper, is relatively independent of deformation temperature and is approximately 7 MPa at a strain of 0·017, rising to approximately 17·5 MPa at a strain of 0·067. That σ_0 is relatively small is also shown by Hutchison and Pascoe [15]. Flow-stress/cell-size relationships may be obtained in two ways: either by plotting log σ *v.* log d, from which a direct measurement of n may be obtained (provided σ_0 is negligible) or, by plotting σ *v.* d^n (assuming various values of n) and obtaining a straight line of best fit through a low value of σ_0. Both of these plots were made: the log σ *v.* log d curves are shown in Figure 10. At 196, 293 and 373K, the results could lie partly on straight lines for strains greater than 1. (The strain of 1 is probably that above which the cellular structure has been well-formed and is a dominant parameter affecting flow stress.) The gradients of the lines in Figure 10 are not the same; approximate gradients (and n values), where the temperature of testing was the same as the temperature of deformation, were $-0{\cdot}62$ at 196K and $-0{\cdot}11$ at 293K. Various σ *v.* d^n curves are plotted in Figure 11; the appropriate n for best fit agreed with that obtained using log-log curves.

The exponent n also varied if the flow stress was measured at a temperature (T) different from the deformation temperature (T_d). For $T_d = 293$K, there was a decrease in n as T decreased, from $n = -0{\cdot}11$ at $T = 293$K, to $n = -0{\cdot}28$ at $T = 77$K; also for $T_d = 373$K, $n = -0{\cdot}15$ at $T = 373$K and decreased to $-0{\cdot}33$ at $T = 77$K. For $T_d = 196$K, however, there was no change in n within experimental error.

For $T_d = 196$ and 293K and for the lower cell sizes (i.e. higher strains), there was also some indication that the gradient on the log σ *v.* log d plot was becoming larger in magnitude.

3.5 Internal Cell Diameter

The results obtained using the Quantimet gave an estimate of the area of the cross-section of the wire occupied by dislocation walls and tangles. In the first instance, the ratio of A_w/A_0 was obtained, where A_w is the area of tangles and A_0 is the area of the detecting frame of the Quantimet. It should be noted that the cell diameter d (as discussed above) is a mean linear intercept value, which includes the dislocation wall thickness (w) together with the diameter of the dislocation-free area of a cell d_f.

Using the above definitions, the total area of dislocation-free regions is $(A_0 - A_w)$, and the

total number of cells per detecting frame is

$$4A_0/\pi d^2, \text{ approximately}$$

and,

$$d_i = (1 - A_w/A_0)^{0.5} d, \text{ again approximately.}$$

The values of A_w/A_0 for various deformation temperatures were obtained as a function of strain and are shown in Figure 12; also shown are the standard deviations for each point, and a smooth curve through the points. As seen above, the calculated value of d_i depends on the measured values of d and A_w/A_0, the latter quantity having a relatively large error. Therefore, the value of d_i is calculated both from actual measured values of d and A_w/A_0 and also values taken from the smoothed curves of Figures 12 and 8. Both these values were plotted as a function of deformation and incorporated in Figure 8, which shows that d_i tended to approach a limiting value more rapidly than d.

Only at 293K is there a wide enough range of d_i to allow a fully defined log σ *v.* log d_i relationship (Figure 10(*b*)). However, at 196K a relationship between log σ and log d_i is found that is qualitatively similar to that at 293K, though over a narrower range of d_i values (Figure 10(*a*)). It is seen that d_i is relatively constant at $0{\cdot}175 \pm 0{\cdot}01$ μm while the flow stress (σ) changes from approximately 470 to 600 MPa.

The ratio of the area of cell interior (A_c) to the area of dislocation tangles (A_w) was also calculated. Figure 13 shows that this ratio increased fairly linearly with increasing deformation, for deformation temperatures between 196 and 373K, though for 293K a smooth curve was a more accurate fit to the points. When A_c/A_w is plotted against flow stress (Figure 14), it is seen that at 293K the flow stress entered a region of low work-hardening rate, but the cell walls continued to refine. A similar constant flow stress was reached for the deformation temperature of 373K, but not quite so clearly; however, at 196K the flow stress and A_c/A_w continued to vary almost linearly.

4. DISCUSSION

4.1 Dynamic Recovery and Recrystallization

At all temperatures, it is seen that, upon deformation by drawing, the initially annealed, equiaxed copper rod (grain size $28{\cdot}2$ μm) rapidly acquires dislocation tangles that delineate cells of lower dislocation density. As deformation continues, these cells refine and become much more definite. The strain at which the cell becomes clearly defined depends on the temperature of deformation; and decreases as the temperature increases. This dependence is characteristic of a thermally activated recovery process, in which dislocations are able to move sufficiently easily and rapidly that a cellular structure forms, as predicted theoretically by Holt [1], and shown experimentally by others [6, 16]. Even though the recovered structure predominates, the second type of cell boundary (section 3.1) observed (Figure 4), appears to be associated with much higher angular misorientations between neighbours. This higher misorientation is shown by the greater contrast between neighbouring cells than that at lower strains (e.g. Figure 2(*b*) c.f. Figure 2(*i*) and Figure 1(*a*) c.f. Figure 1(*e*)) and also by selected-area diffraction. The structure of the boundary is also different, in that the dislocation density appears much higher than for the boundaries which first appear at lower strains.

The definition of recovery, polygonization and recrystallization has been discussed by many writers [17, 18, 19, 20]. In the absence of further evidence, arbitrary definitions, e.g. that misorientation between grains of greater than 5 degrees indicates recrystallization, have been used. Recrystallization occurring during deformation is often referred to as dynamic recrystallization. Much work has been done on highly deformed copper and nickel, though usually at elevated temperatures and by torsion [21, 22, 23]. These torsion experiments were usually performed in such a way that the metal was quenched to a lower temperature, either immediately before or just after cessation of deformation. Microstructures observed after such procedures show [24] a well-developed network of fine equiaxed grains subdivided by cell walls. These new, equiaxed grains are thought to arise by a process of dynamic recrystallization, in which new grains form during deformation, out of a collection of dislocation cells.

An important difference between the shape of grains found in copper deformed at 1073K by torsion and the cells or grains in copper deformed at 196 to 473K by drawing, is that the former are equiaxed, while the latter are elongated (Figure 6). The fact that the drawn grains are elongated need not, however, preclude them from forming by a recrystallization process. A high-voltage electron microscopy study of rolled copper by Ray *et al.* [25] showed that new grains, formed during heating, tend to develop as colonies, or strings, of recrystallized grains. If a recrystallization process is occurring during drawing, the new cells or grains need not be equiaxed (as they would tend to be if produced by thermal annealing) but could be elongated along the wire, as has been observed with cells in extruded aluminium rods [22]. The elongated grains apparently occur because of the way in which the wire is deformed. Just prior to the wire entering the die, most of the internal energy is in the form of thermal energy (approximately $3RT$), plus the stored deformation energy obtained during the previous passes. During drawing, the wire diameter is reduced, work is done on the metal and the internal energy rises. In high stacking-fault-energy metals such as aluminium, the activation energy for recovery processes is sufficiently low that dynamic recovery occurs during the deformation, thereby maintaining the cellular microstructure. For lower stacking-fault-energy metals such as copper, the activation energy for recrystallization is similar to that for recovery, and may even be lower [26]. This result leads to the explanation that dynamic recrystallization can produce the microstructures formed during hot working.

In the higher internal energy regions of the wire, there will be certain drawing conditions of temperature, strain rate and stored deformation energy, at which the metal may reduce its energy by dynamic recrystallization, rather than by dynamic recovery. The metal rod, or wire, effectively sees an internal energy "hot spot" passing along its length, similar to that during the hot zone technique of single-crystal growing. The passage of this high energy region along the wire could produce highly elongated new grains as shown in Figure 6.

The changes in internal energy observed during thermal annealing of copper and aluminium [27] indicate that, in copper, over 90% of stored deformation energy is not released until recrystallization occurs, whereas, in aluminium up to 50% of the stored energy is released during the recovery stage. These figures show that more stored energy is available in copper, than in aluminium, to add to the existing thermal energy, thereby assisting recrystallization during deformation at lower temperatures in copper than in aluminium.

The possibility of dynamic recrystallization and dynamic recovery occurring together allows an explanation for the two types of boundary observed in the electron micrographs (Figures 1, 2, 3, 4). Here, the sharply defined boundaries are attributed to dynamic recrystallization and the loose dislocation-tangle boundaries to dynamic recovery. Recrystallization is also more likely as the temperature increases, thus explaining the increasing incidence of the sharp boundaries as deformation temperature is increased. Recrystallization considerations could also explain the increasing fraction of ⟨100⟩ texture in copper, at a given strain, with increasing deformation temperature [28]. The ⟨100⟩ texture arises from the well-documented [29, 30] property of face-centred-metals to recrystallize into the cube orientation.

Further evidence consistent with dynamic recrystallization occurring is provided by the tensile stress-strain curves of the drawn wires, especially at 373 and 473K [31] (Figure 9). During drawing, the wire initially continues to work-harden up to a certain strain, but for each drawing strain increment thereafter the wire softens. The total strain at which the flow stress starts to fall decreases as drawing temperature increases. Analogous decreases in flow stress during torison and extrusion of aluminium, nickel and copper have been explained in terms of dynamic recrystallization [21, 23].

The strain to reach peak flow stress is expected to approximate closely the critical strain at which the stored energy is sufficiently high for the metal to recrystallize during deformation. As deformation proceeds, so also does recrystallization and, due to the requirement of compatibility of strains between adjacent regions, the overall flow stress is now an average over the specimen of all regions, ranging from newly recrystallized grains (with very low flow stress), through to deformed grains and cells (intermediate flow stress), to highly deformed cells that are just about to recrystallize (maximum flow stress). Eventually a constant equilibrium flow stress is approached. The result of this sequence of events is consistent with microstructural observations (e.g. Figure 4) where the recrystallized grains contain regions of high dislocation density, together with a regular array of loose walled cells. Here, recrystallization could not have occurred after drawing, since the cell structure inside the deformed grains would have been lost during recrystallization and replaced by unstrained new grains and annealing twins.

These results are consistent with the interpretation that, during deformation of copper by wire drawing, there is a close competition between dynamic recovery and dynamic recrystallization and these related processes occur concurrently. Even at 196K, there is evidence (Figure 1) of new grains formed by dynamic recrystallization, though the bulk of the microstructure consists of cells formed by dynamic recovery. Evidence of dynamic recrystallization in copper at temperatures as low as 196K has not previously been reported, nor has the elongated nature of the dynamically recrystallized grains (length-to-diameter ratio greater than 7) (Figure 6), although recrystallization has been suggested after drawing at 293K [17].

4.2 Cell Size and Dislocation Density

That copper and other metals approach a limiting cell size as deformation proceeds (Figure 8) has also been shown by other workers [6]. A constant cell size independent of further deformation can be achieved in at least two ways. The first is one in which the long cells, having once been formed, maintain their identity and slide over each other during deformation like straws in a bundle (much akin to superplastic deformation theories). This process is likely to need a high activation energy to enable sliding to occur, since the boundaries are very "rough" compared with normal grain boundaries. The temperatures are also too low for the necessary diffusion to occur as with normal grain boundary sliding (e.g. during superplastic deformation). The second process, leading to constant cell size, is one in which a highly dislocated structure is formed during deformation and then dynamically recovers to form cells, as suggested by Holt [1]. A result of this mechanism is that each cell need not continue as a definite entity, from one wire-drawing pass to another, but becomes part of a general tangle of dislocations which dynamically recovers to the cell structure. Holt concludes that the cell diameter (d) is given by the wavelength (λ) of the modulation of the dislocation density (ρ), and that λ is proportional to $\rho^{-0.5}$. A basic assumption of his derivation is that the dislocation mobility is sufficient for the lowest energy configuration to be approached, i.e. that the processes of dynamic recovery can proceed and thereby govern the dislocation structure.

From the results of cell size v. strain (Figure 8), it can be concluded that, since a limiting cell size is reached at 196K, 293K and 373K, the dislocations are mobile enough for dynamic softening processes to occur. The additional cross-sectional density of dislocations necessary to accommodate a strain of 0·25 (per wire drawing pass) is at least 10^{14} m/m^3 and can be much higher, e.g. when the expansion of dislocation loops is hindered by barriers or dislocation tangles [32]. In copper, if the average dislocation moved through the tangle a distance of 1 μm, the expected dislocation density would be approximately 2.10^{17} m/m^3. However, after heavy deformation, the dislocation density saturates in the region of 10^{16} m/m^3 in most metals [32]. Thus, it appears that the limiting dislocation density is probably a more relevant parameter in deformed metals than the limiting cell size, especially if recovery processes are operating. It is therefore likely that, once a high dislocation density has been obtained, the number of dislocations available to recover dynamically is relatively independent of the temperature and/or total strain, in which case the modulation wavelength (λ) and cell size (d) will also be relatively independent of temperature and total strain. Such independence of increased dislocation density with temperature and strain would explain why the cell sizes at 196, 293 and 373K come to a similar value (0·21 ± 0·03 μm) over a wide range of true strain, especially as shown for 196 and 293K (Figure 8).

4.3 Flow-Stress Relationships

The variations of flow stress with mean linear intercept dimension (M.L.I.) (i.e. the diameter of a cell measured from the centre of the dislocation wall) and the diameter of the dislocation-free zone (d_f) (Figure 10) for 196 to 373K, can be divided into three regions, viz.:

(i) low strain (unformed cells and/or large cell size)
(ii) medium strain (well-formed cells)
(iii) high strain (well-formed) cells).

Region (*i*), occurring for strains below 1, has a gradient on the log σ v. log M.L.I. curve much greater than the gradient in region (ii). This difference is probably due to the presence of large-scale dislocation tangles and the poor formation of cells at low strains. As strain increases and the cells become better defined, an approach to a linear relationship is observed. This linear relationship is consistent with a Hall-Petch type relationship although only at 196K is the gradient of the

same magnitude as previously found [4, 6], i.e. n approximately $-0{\cdot}6$. For deformation at 293 and 373K, the gradient of the linear part of the curve is much lower (n approximately $-0{\cdot}1$ to $-0{\cdot}3$, depending on the temperature of testing). The lower magnitude of n at higher deformation temperatures could be due to the competing processes of dynamic recovery and recrystallization. The latter process will form cells or new grains of lower flow stress, thus causing the average flow stress to be lower. The lower flow stress will be due not only to any lower dislocation density in the new grains, but also to the tendency for recrystallization to form a ⟨100⟩ texture along the wire axis [28]. The grains of ⟨100⟩ orientation have a lower flow stress than the cells or sub-grains of ⟨111⟩ texture, which is the second component of the duplex texture produced during drawing of copper. (The dependence of n on the temperature of testing, for 293K and 373K wires, may also be due to the presence of the second type of boundary produced at higher temperatures, or the increased "transparency" of these walls to other dislocations at higher temperatures, especially if penetration is a thermally activated process.)

The third region of interest in the log σ *v.* log M.L.I. curve occurs when the limiting cell size has been reached and the flow stress continues to change. At 196 and 293K, the flow stress increases, but at 373 and 473K the flow stress decreases (at 373K, this decrease is not seen in Figure 10(*c*) but is shown in Figure 9). The continued change in flow stress at limiting cell size is thought to be due to the continuing formation of texture with continued deformation [28, 31, 33]. At 196 and 293K, the increasing ⟨111⟩ texture tends to increase flow stress, whereas at 373 and 473K, the ⟨100⟩ texture increases with deformation and, as it has a lower flow stress than ⟨111⟩ orientations, causes a decreasing average flow stress. At 473K, the softening due to the ⟨100⟩ texture is accompanied by softening due to the increasing cell size of the recrystallized grains (Figure 8(*d*)).

4.4 Changes in Thickness of Cell Walls

A decreasing fraction of the specimen is occupied by dislocation walls and tangles as deformation increases at the three temperatures for which this effect was studied (Figure 12). There is no evidence that the area of cell walls or tangles (A_w) has reached a limiting fraction of the total area (A_0), even at quite high strains, although the curve is monotonically decreasing with increasing strain. These changes indicate that, since the cell size M.L.I. has remained relatively constant over this strain interval, the cell walls must be refining and becoming thinner as the specimen is deformed. This conclusion is reinforced by the increasing ratio of the area of the cell interior to the area of cell walls (A_c/A_w) with increasing strain (Figure 13). The linear, or near linear, relation of A_c/A_w with strain means that the wall area is becoming a less significant fraction of the total specimen cross-sectional area.

Using the ratio of wall area to the specimen area, the internal diameter of the cell can be calculated and plotted as a function of strain as shown in Figure 8. The internal diameter tends to a limiting value in a way similar to the M.L.I. The limiting value of the internal diameter (d_i) occurs at a lower strain than for the M.L.I.; in fact, at 196 and 373K, d_i is almost constant at all strains investigated. The plot of log σ *v.* log d_i (Figure 10) therefore indicates that the flow stress is much less dependent on d_i than on the overall M.L.I. The three regions of the log σ *v.* log M.L.I., indicated in Section 4.3, also occur in log σ *v.* log d_i plots, and the same reasons apply for their occurrence.

5. CONCLUSIONS

It has been shown that the dislocation cells, which presumably result from a need to minimize total dislocation free energy, reach a limiting size that is relatively independent of strain and deformation temperature. This limiting size may be governed by the limiting dislocation density observed in most heavily deformed metals. Although the cell size remains relatively constant at high strains, the morphology of both the cell walls and cell interiors continues to change, in that the volume of dislocation walls decreases and the cell interiors become increasingly free of dislocations. The rate at which these changes occur increases at the deformation temperature increases.

No single parameter was found to determine the flow stress at all strains. At low strains, before of just after dislocation cells form, the dislocation density (ρ) may be measured. It has been shown

to be related to flow stress (σ) by $\sigma \propto \rho^{0.5}$ [1].

At medium strains, dislocation cells form, of a size (d) related to dislocation density, and a power relationship $\sigma \propto d^n$ can be determined; here n is not a universal constant but varies with both temperature of deformation and testing, probably due to the increasing effect of the two types of cell/sub-grain boundaries forming the microstructure. It is proposed that one type of boundary forms by dynamic recovery processes, which predominate at lower temperatures, whereas the other type forms by dynamic recrystallization processes, which predominate at higher deformation temperatures.

At high strains, the flow stress is found to increase despite the constant cell size. The increase (at constant temperature) is ascribed to the increasing influence of texture on mechanical properties. This changing texture could also have some influence on n values, a fact which does not seem to have been considered by other workers.

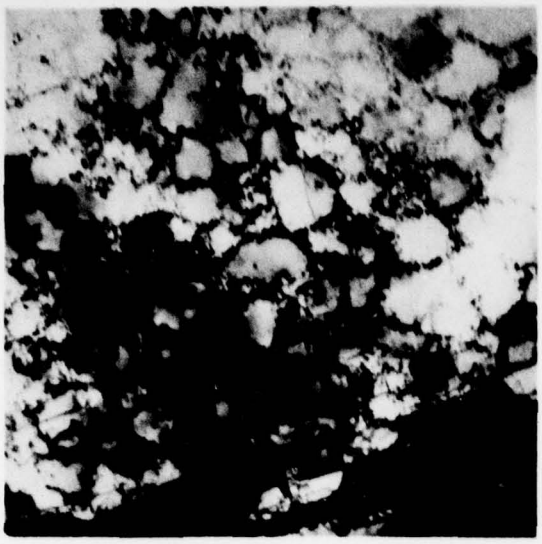

(a) Total strain 0.77

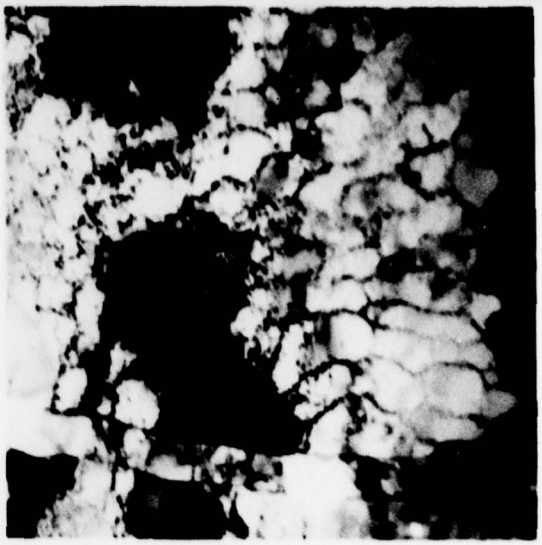

(b) Total strain 1.9

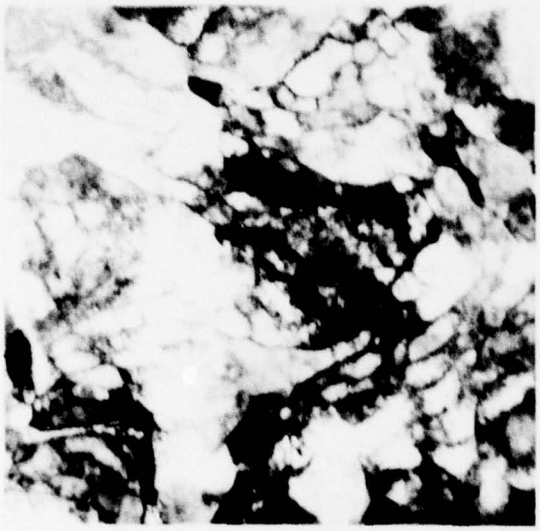

(c) Total strain 2.8

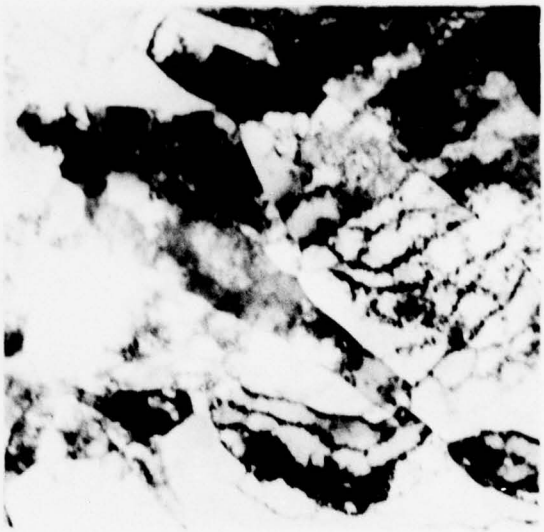

(d) Total strain 3.35

1.0 μm

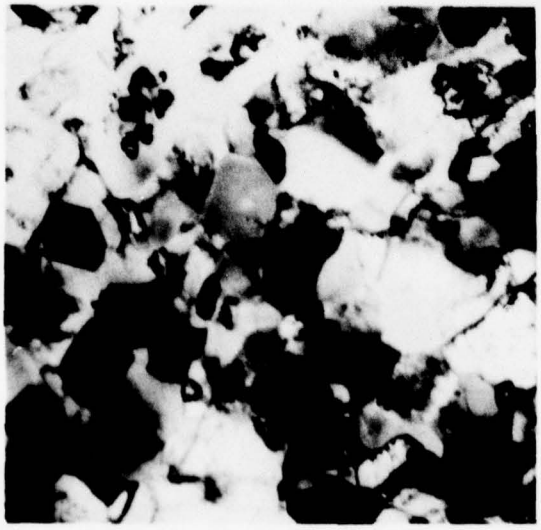

(e) Total strain 6.2

FIG. 1 Dislocation microstructure in copper deformed at 196K. Transverse section.

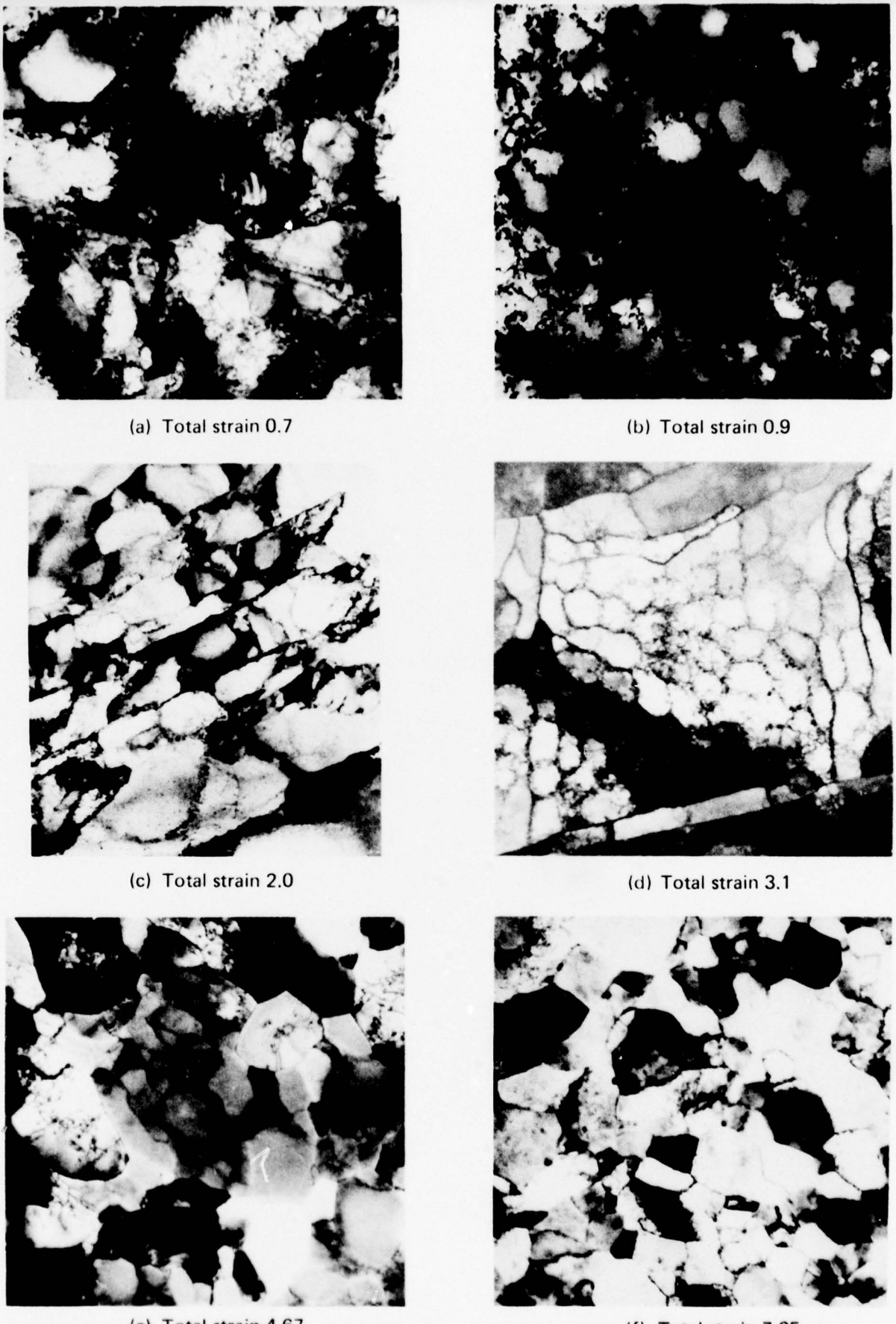

FIG. 2 Dislocation microstructure in copper deformed at 293K. Transverse section.

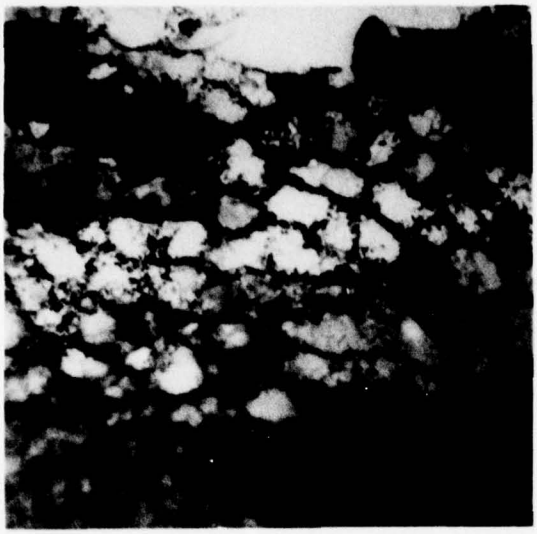

(a) Total strain 0.77

(b) Total strain 1.1

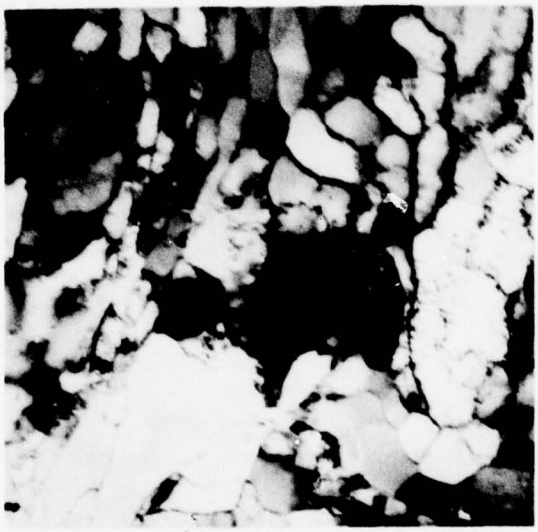

(c) Total strain 2.27

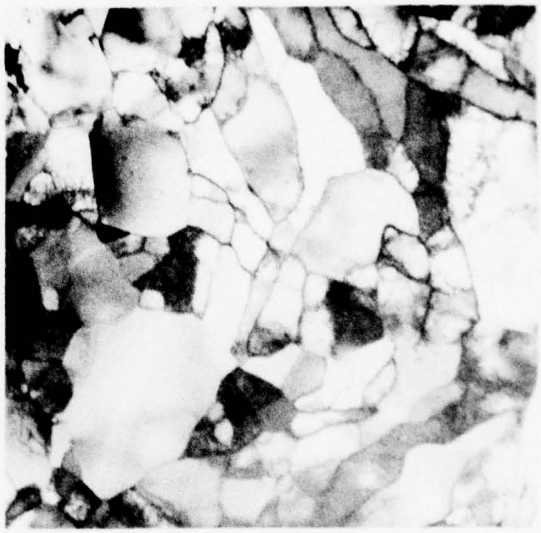

(d) Total strain 2.8

1.0 μm

(e) Total strain 3.04

Fig. 3 Dislocation microstructure in copper deformed at 373K. Transverse section.

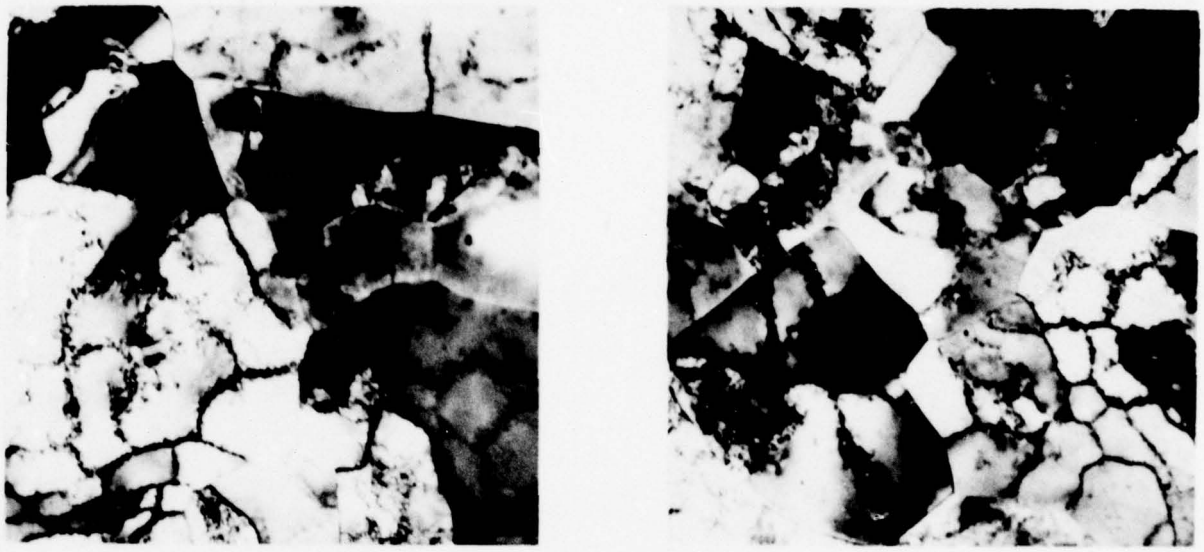

(a) Total strain 0.6

(b) Total strain 3.6

1.0 μm

Fig. 4 Dislocation microstructure in copper deformed at 473K. Transverse section
Both micrographs show the two types of boundary described in section
3.1, viz. those formed by (a) dislocation tangles and (b) sharper higher angle boundaries.

Fig. 5 Dislocation microstructure in copper deformed at 77K, showing area of heavy deformation twinning. Transverse section, total strain is 1.1

Fig. 6 Logitudinal section of copper wire drawn at 473K, to a total strain of 6.2, showing highly elongated nature of the cells.

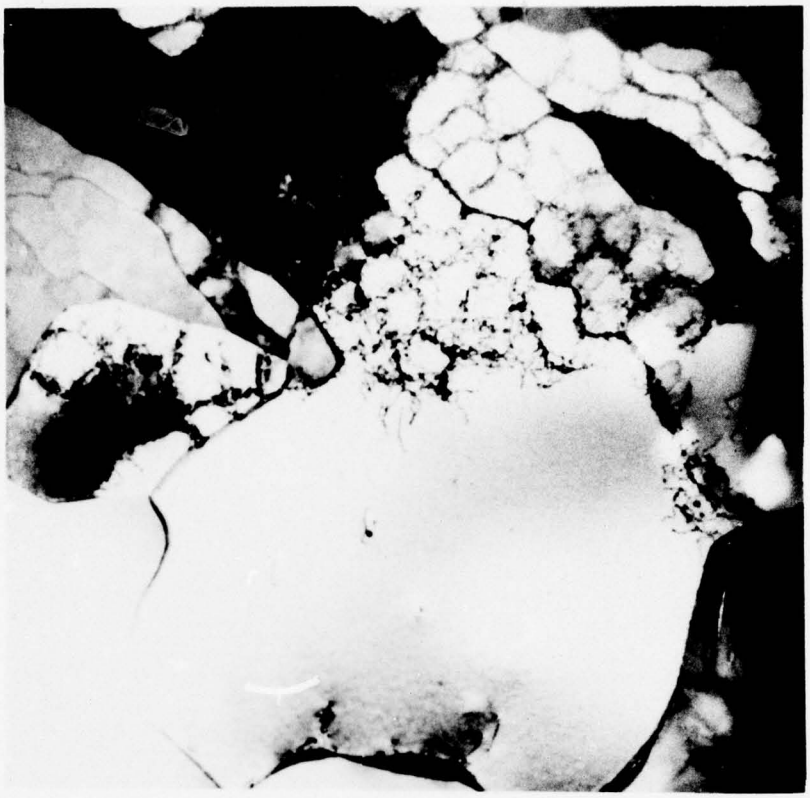

Fig. 7 Transverse section of copper wire drawn at 293K to a total strain of 4.7 and annealed in bulk at 673K for one hour, showing evidence for cell coalescence.

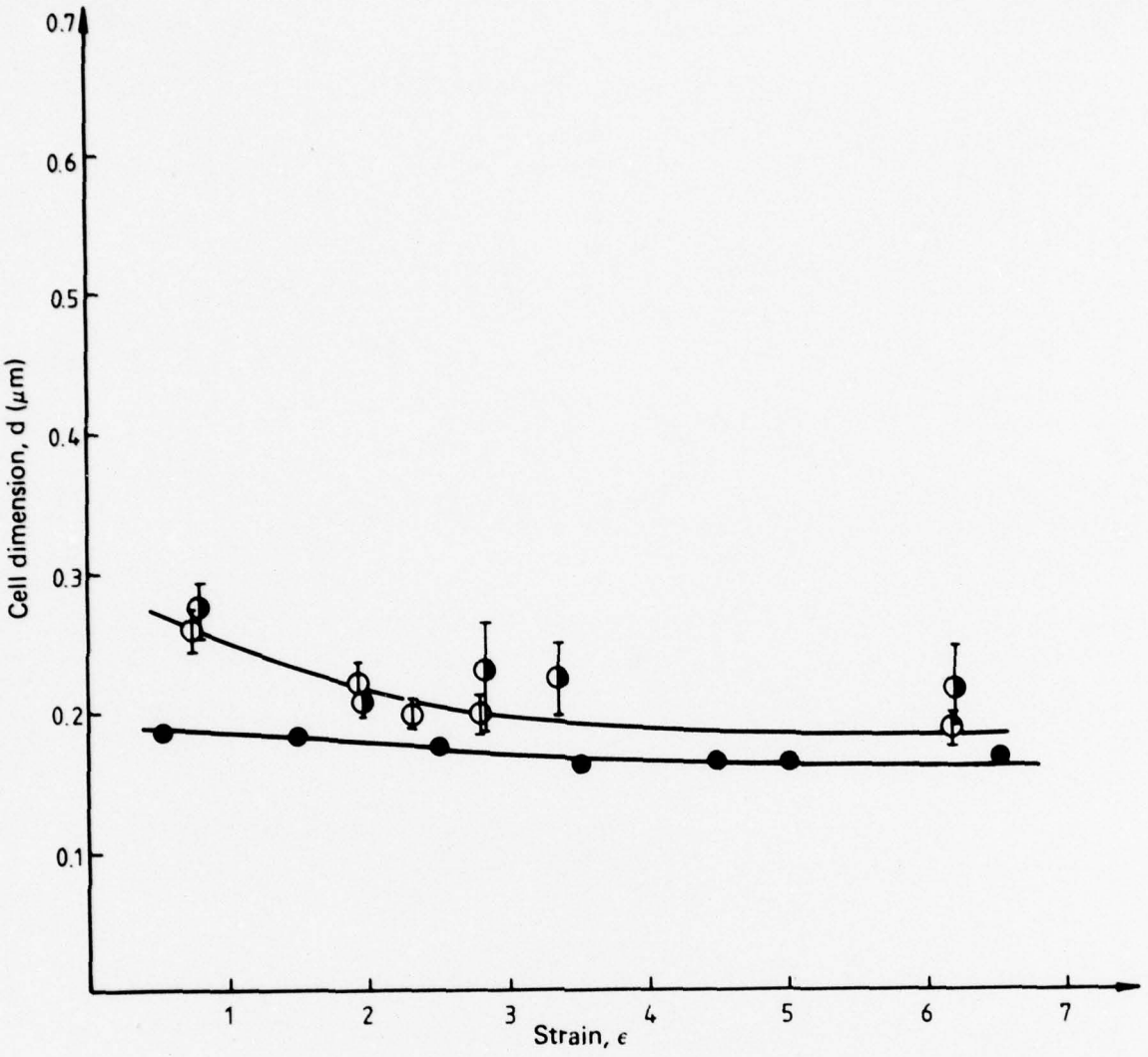

Fig. 8 Mean linear intercept cell size (d) for copper wires as a function of total drawing strain (ϵ). Standard deviations of the mean linear intercepts are also included.
Also shown are the results obtained using the Quantimet, together with standard deviations.
The diameter of the dislocation-free cell interior (d_i) calculated as described in section 3.5 is shown in (a), (b) and (c).
Fully shaded points: d_i obtained from smoothed curves of d vs. ϵ (this Figure) and Figure 12.
Unshaded points: d obtained from direct analysis of electron micrographs.
Half-shaded points: d obtained from Quantimet analysis of electron micrographs.

(a) Temperature of drawing 196K,

○ d vs. ϵ.

◑ d vs. ϵ,

● d_i vs. ϵ.

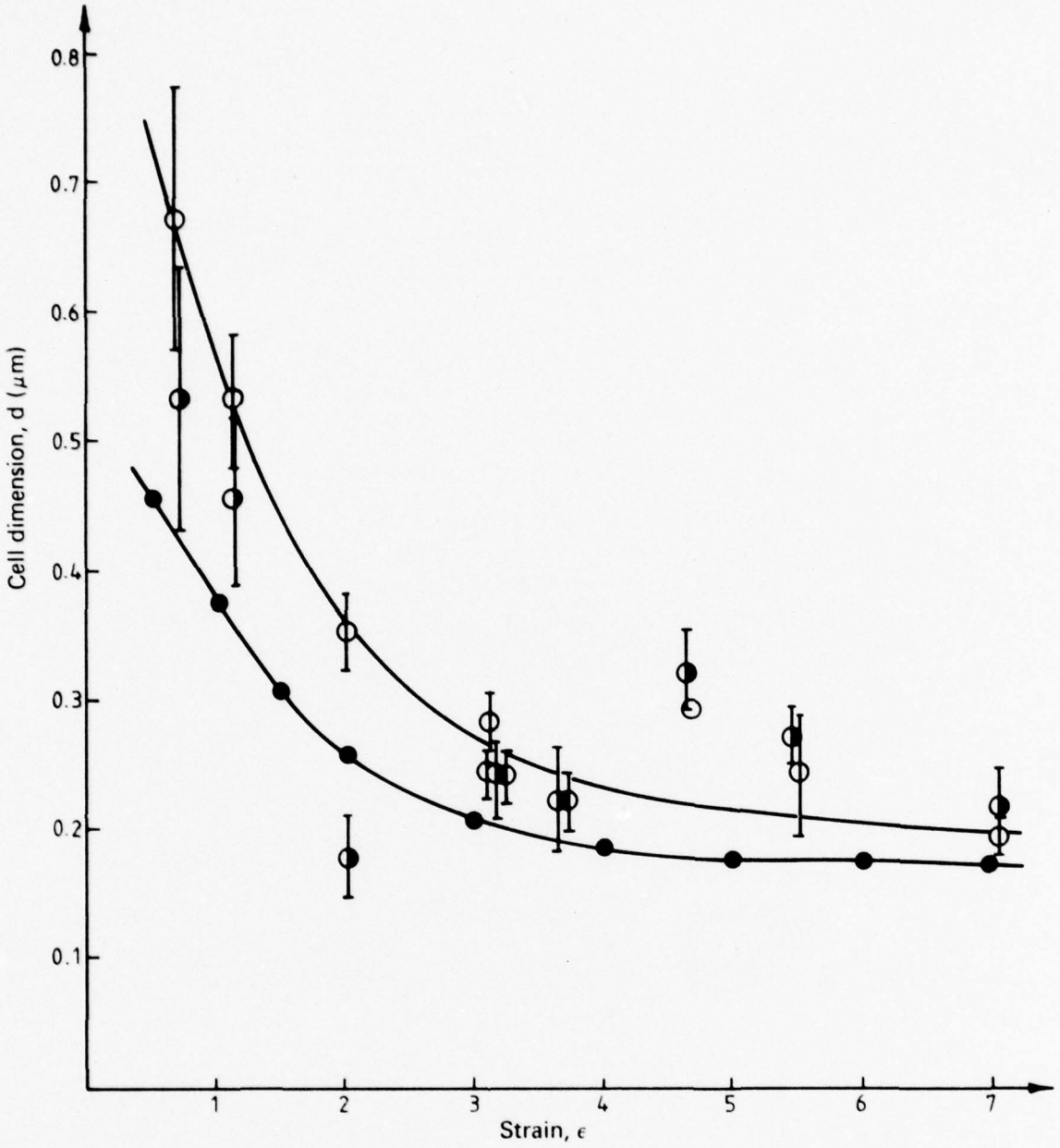

Fig. 8 cont.

(b) Temperature of drawing 293K,

○ d vs. ϵ .

◑ d vs. ϵ .

● d_i vs. ϵ .

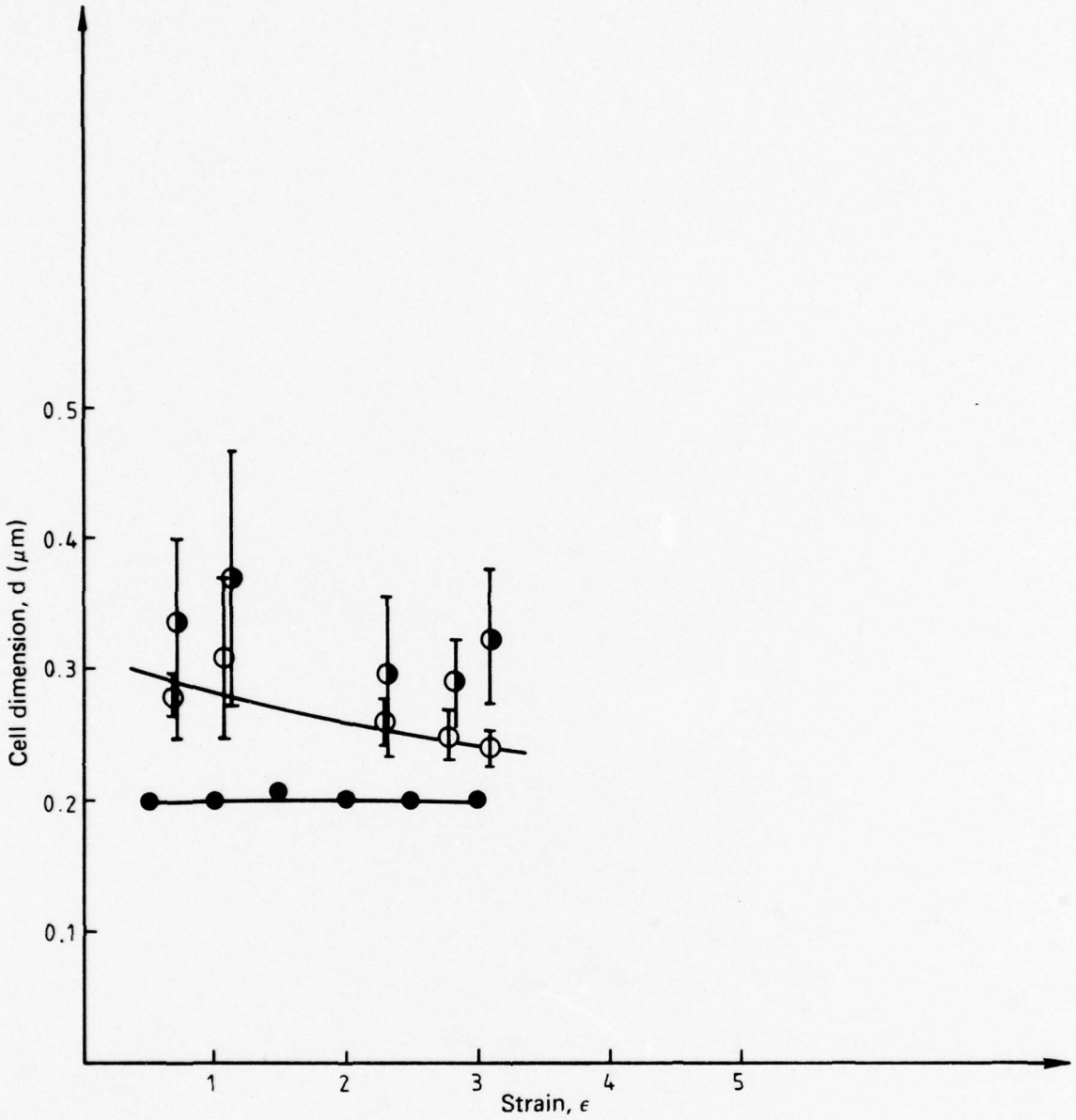

Fig. 8 cont.

(c) Temperature of drawing 373K,

○ d vs. ϵ.

◑ d vs. ϵ.

● d_i vs. ϵ.

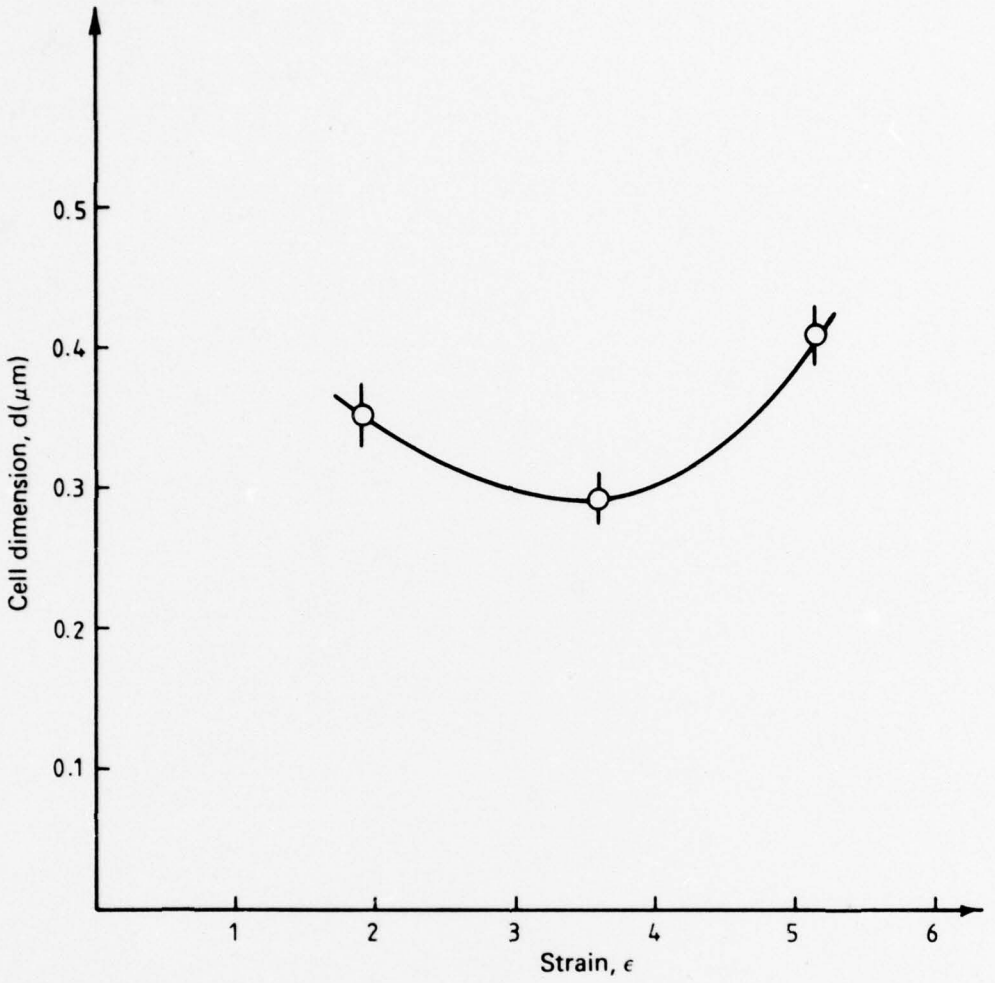

Fig. 8 cont.

(d) Temperature of drawing 473K.

○ d vs. ϵ.

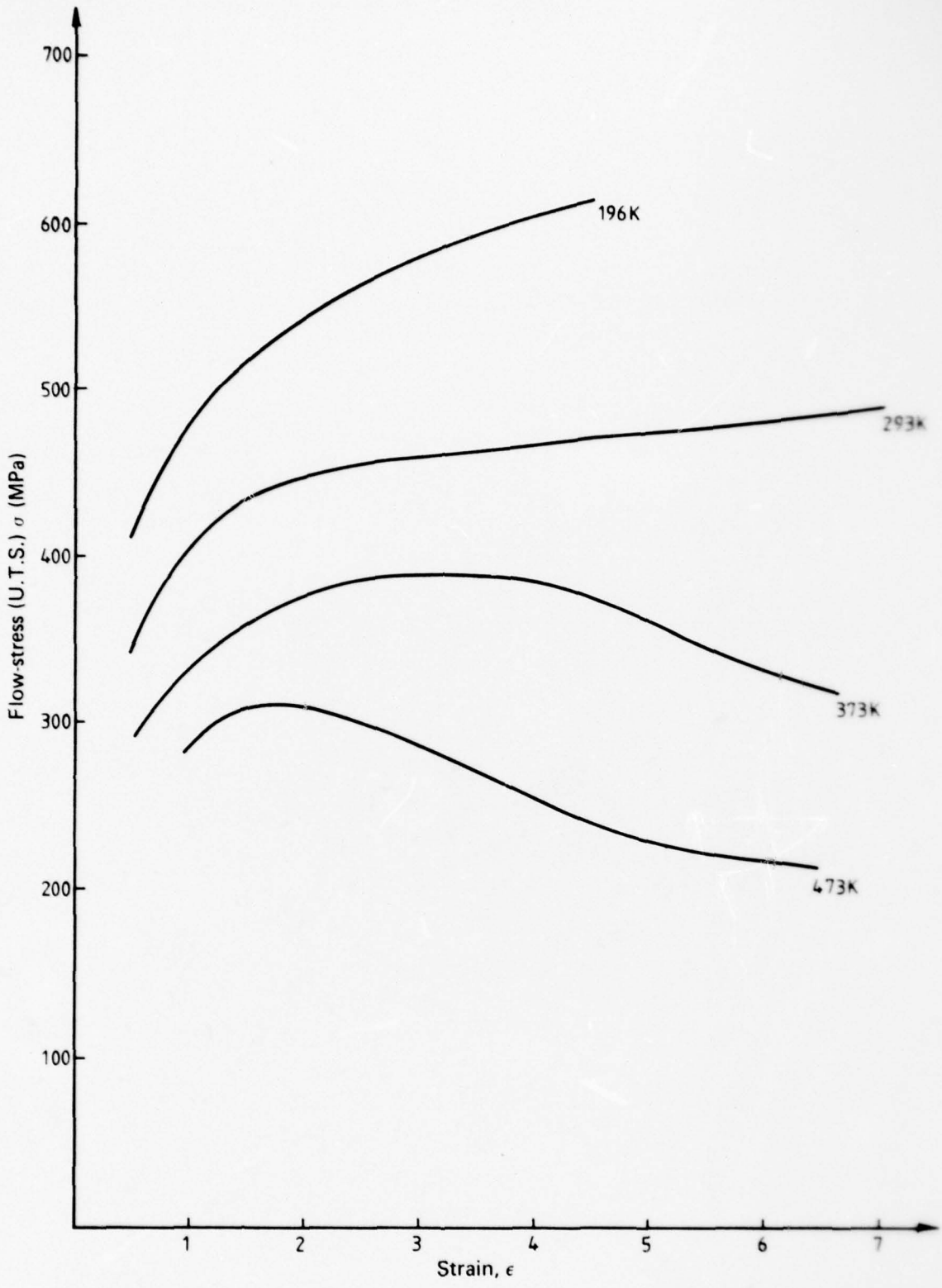

Fig. 9 Typical flow-stress curves for drawn copper wires. The flow stress has been measured at the temperature of deformation as shown.

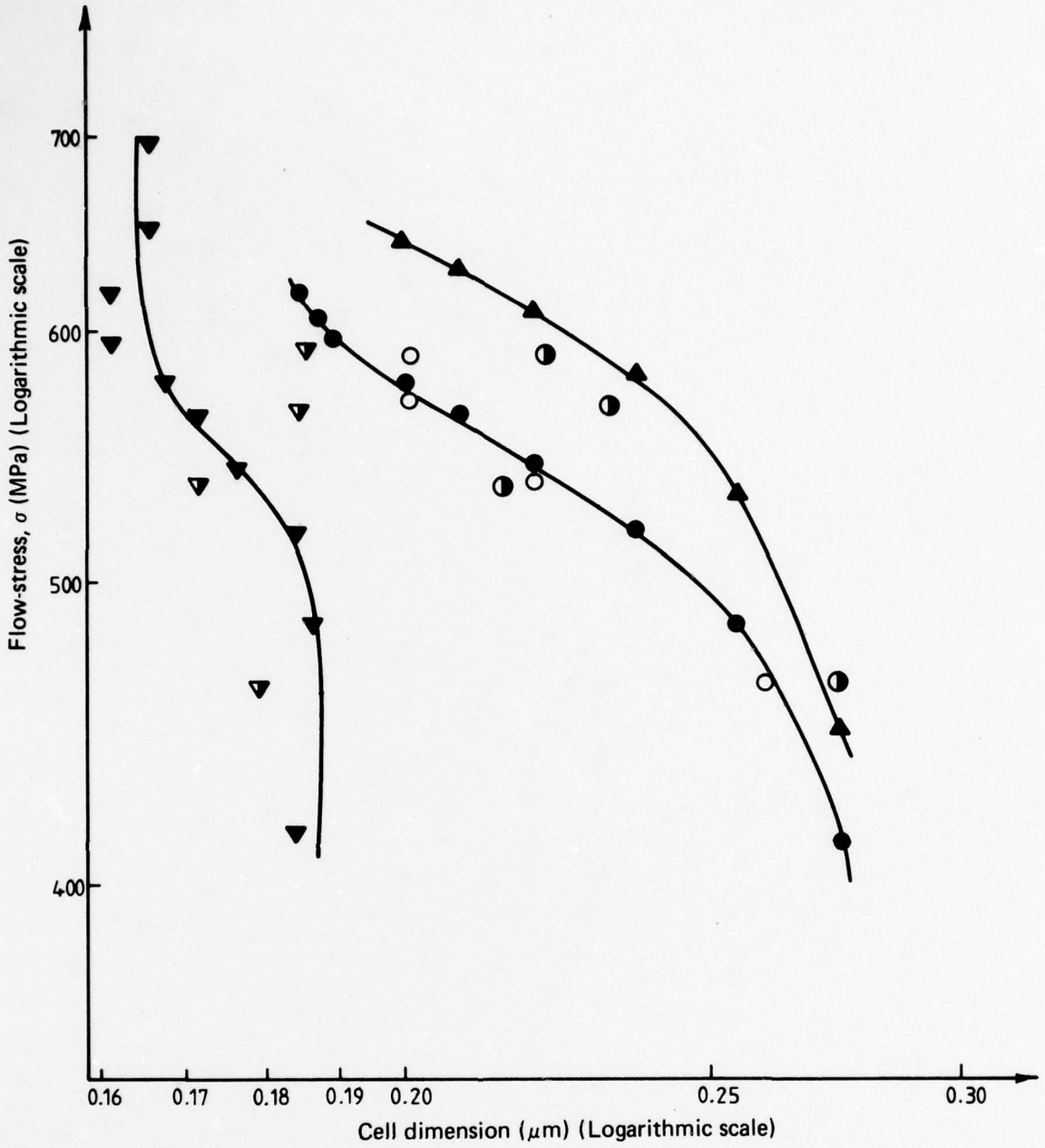

Fig. 10 Flow stress (σ) v. cell size (d) (logarithmic scale) for copper tested at temperatures equal to or less than the deformation temperature.
The internal cell diameter (d_i) is also included as a function of flow stress measured at the drawing temperature.
Fully shaded points: cell dimensions (d, d_i) are obtained from smoothed curves of figures 8 and 9.
Unshaded points: cell dimensions (d, d_i) are obtained from direct analysis of electron micrographs.
Half-shaded points: cell dimensions (d, d_i) are obtained from Ouantimet analysis of electron micrographs.

(a) Temperature of deformation 196K,

○ ● ◑ σ measured at 196K vs. d.

▲ σ measured at 77K vs. d.

▼ ▽ σ measured at 196K vs. d_i

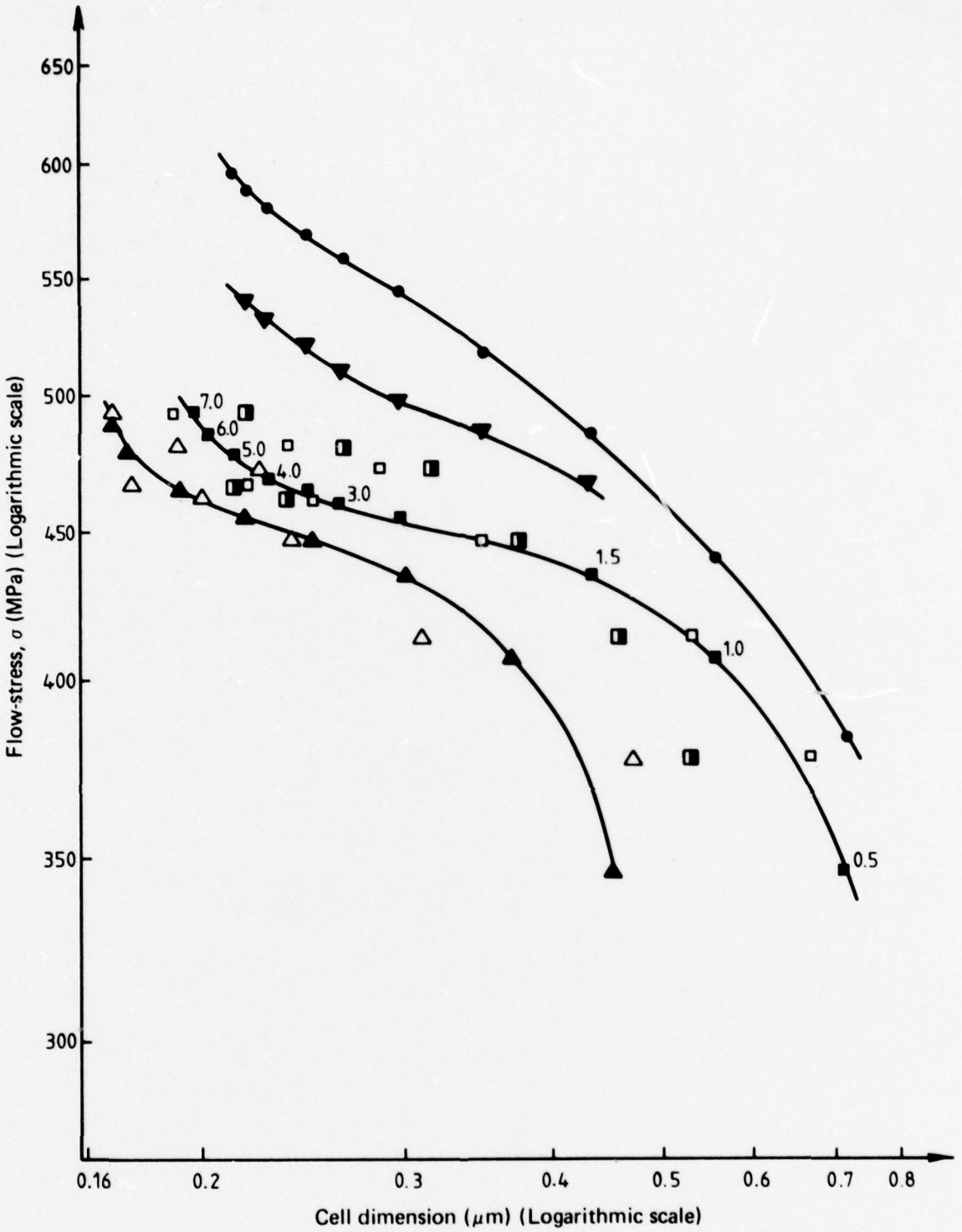

Fig. 10 cont.

(b) Temperature of deformation 293K, (Total Strain indicated on points)

□ ■ ◨ σ measured at 293K vs. d,

▼ σ measured at 196K vs. d,

● σ measured at 77K vs. d,

△ ▲ σ measured at 293K vs. d_i

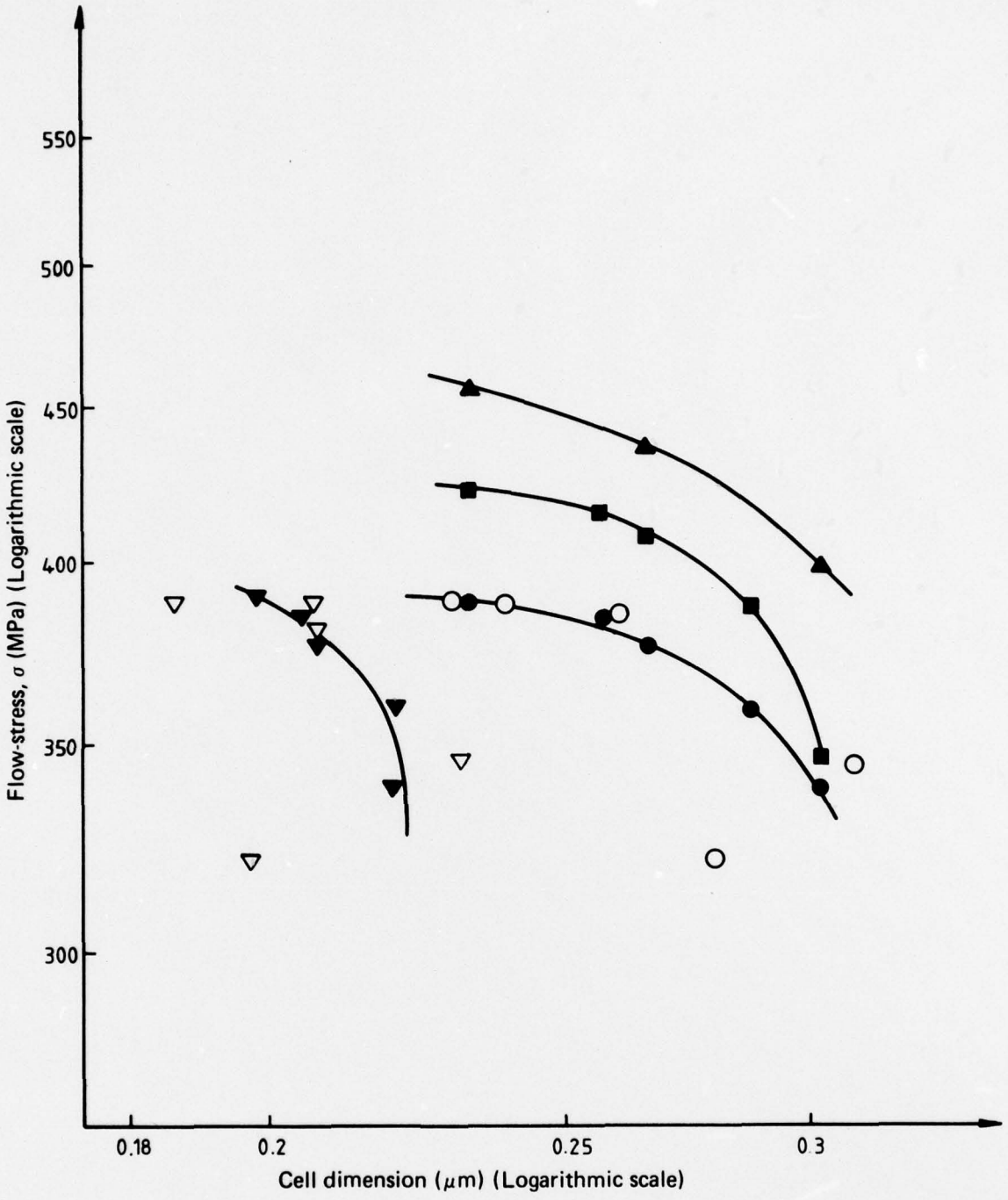

Fig. 10 cont.

(c) Temperature of deformation 373K,

○ ● σ measured at 373K vs. d,

■ σ measured at 293K vs. d,

▲ σ measured at 77K vs. d,

▽ ▼ σ measured at 373K vs. d_i

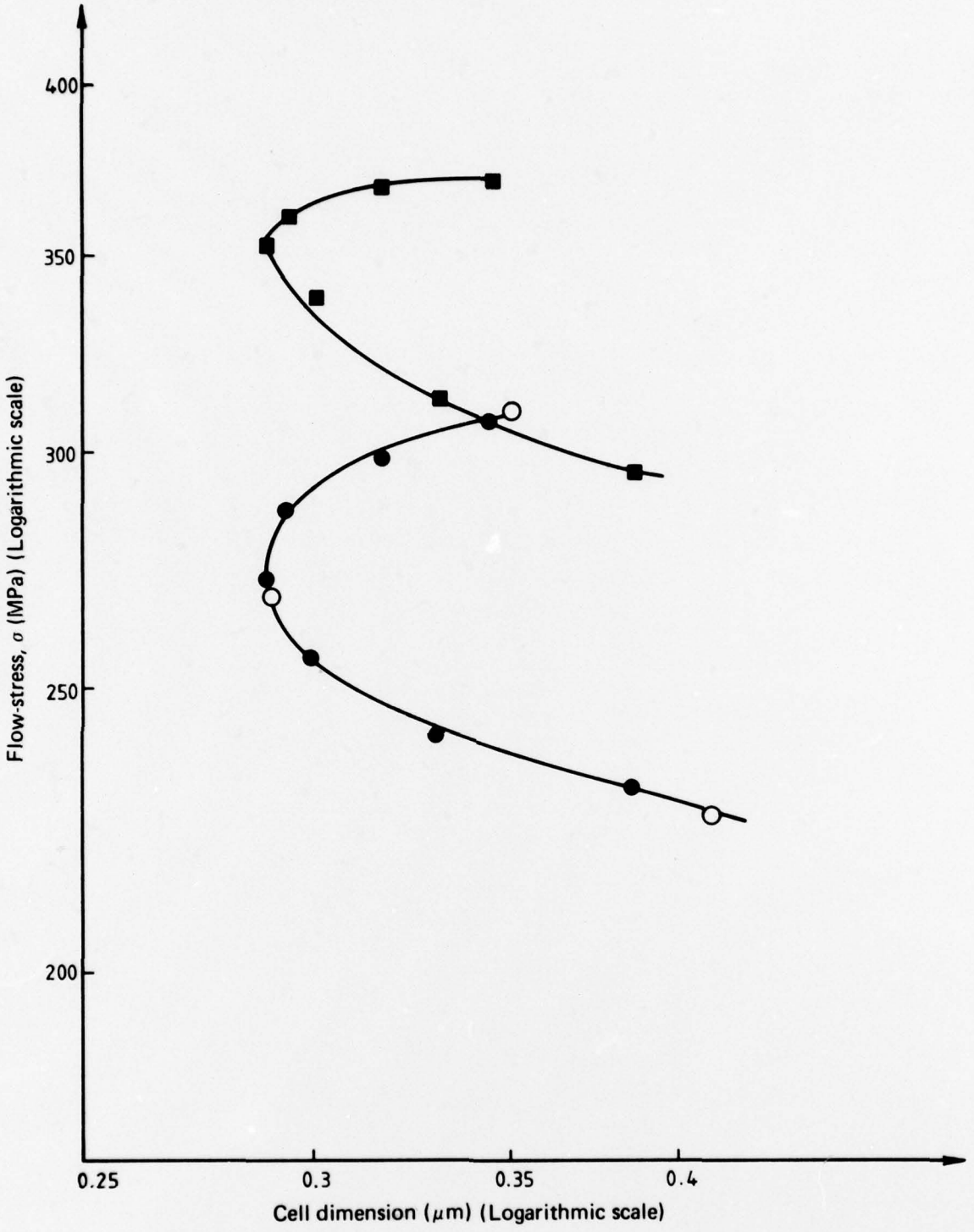

Fig. 10 cont.

(d) Temperature of deformation 473K

○ ● σ measured at 473K vs. d,

■ σ measured at 293K vs. d.

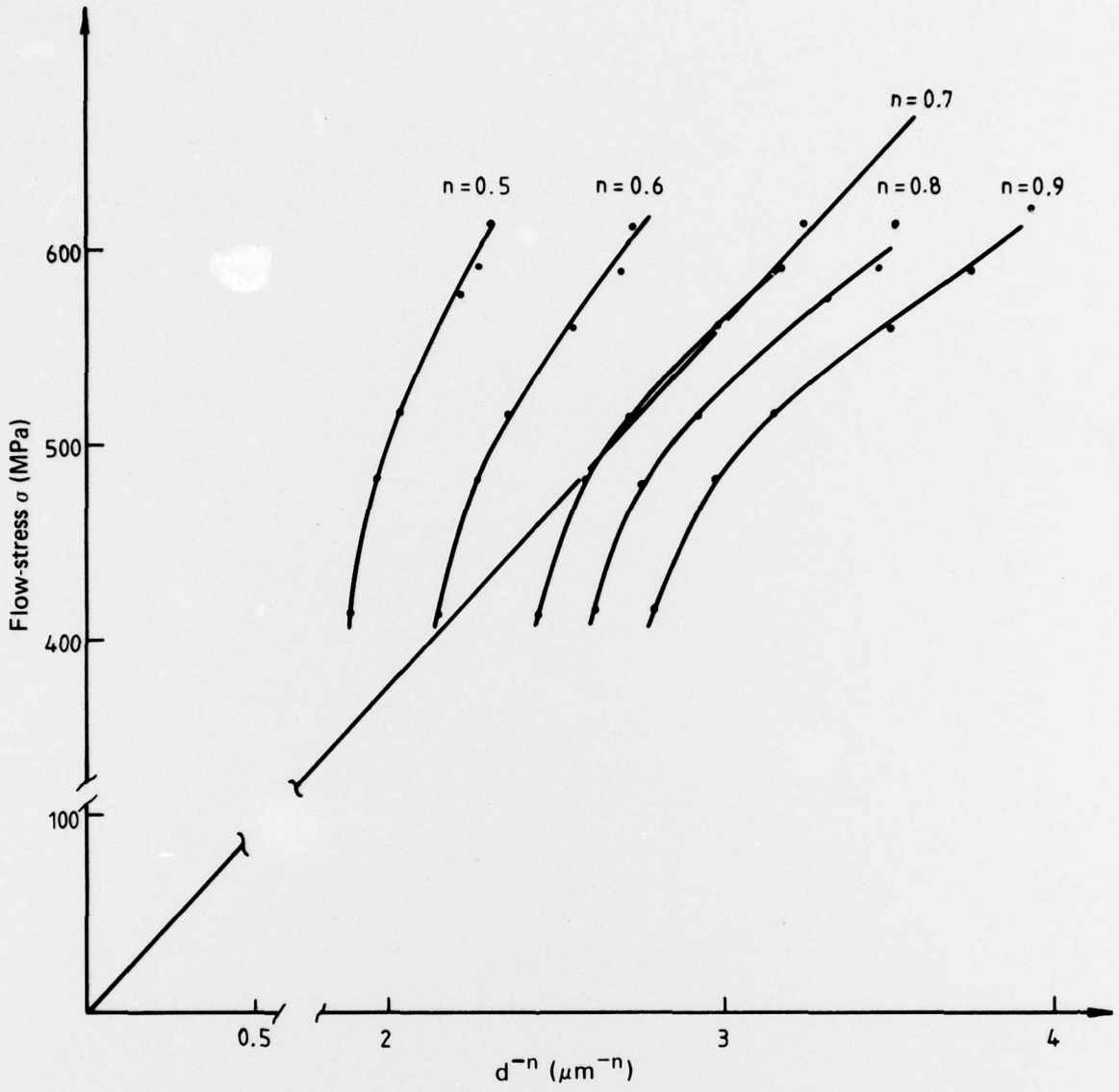

Fig. 11 Flow stress (σ) as a function of cell size (d) where various functions of d^n have been used as the abscissa.

(a) Temperature of deformation 196K

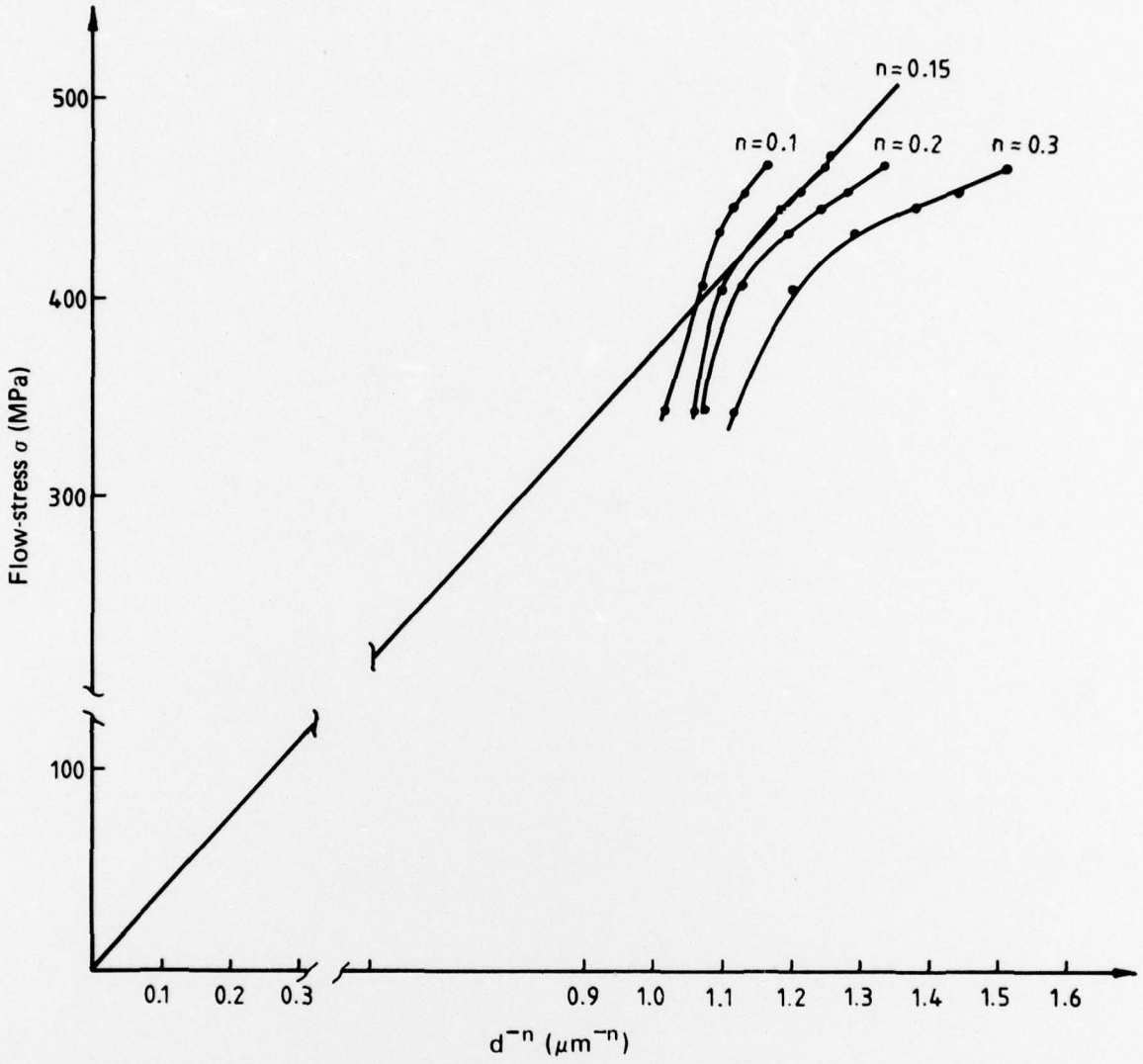

Fig. 11 cont.

(b) Temperature of deformation 293K

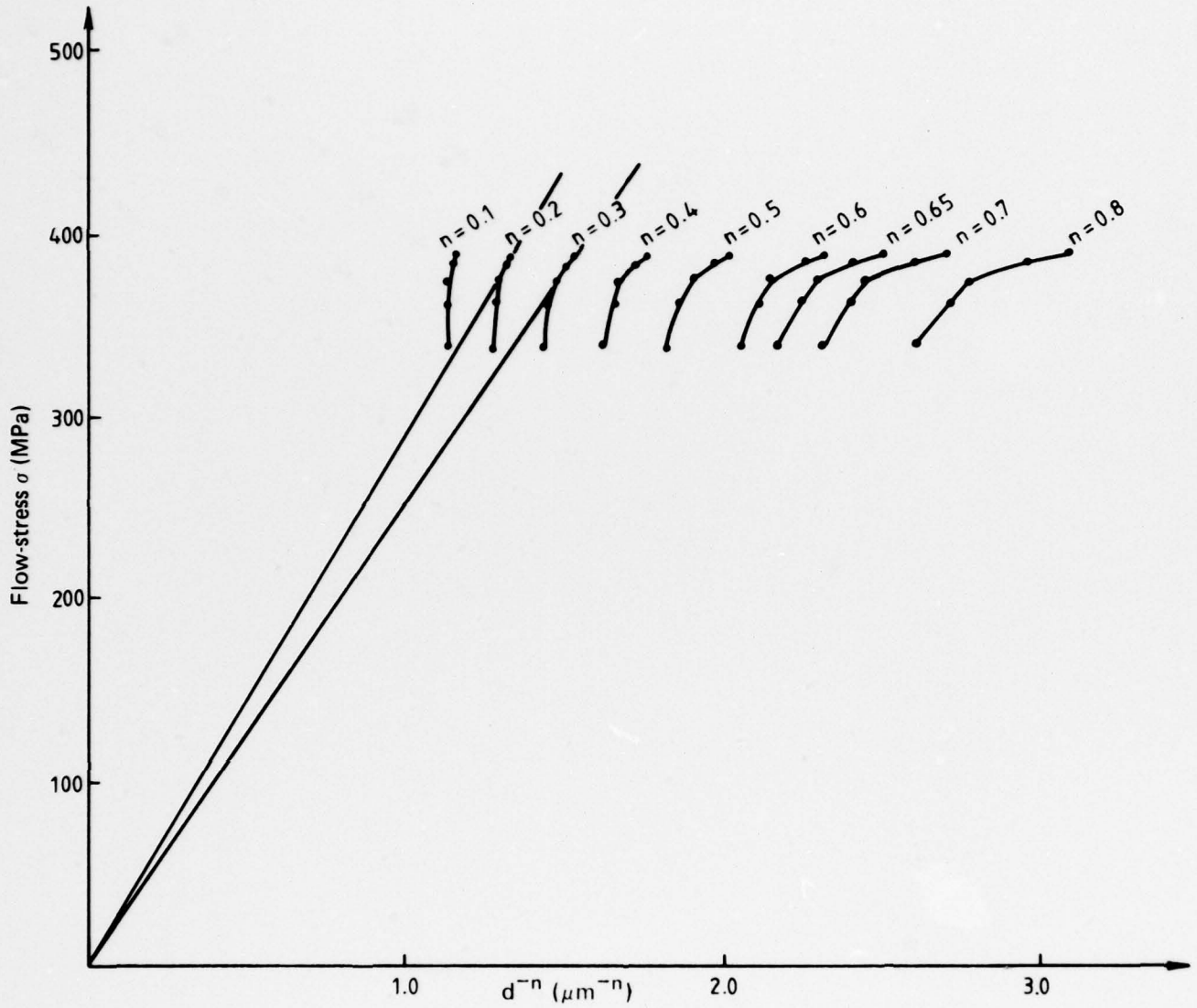

Fig. 11 cont. (c) Temperature of deformation 373K.

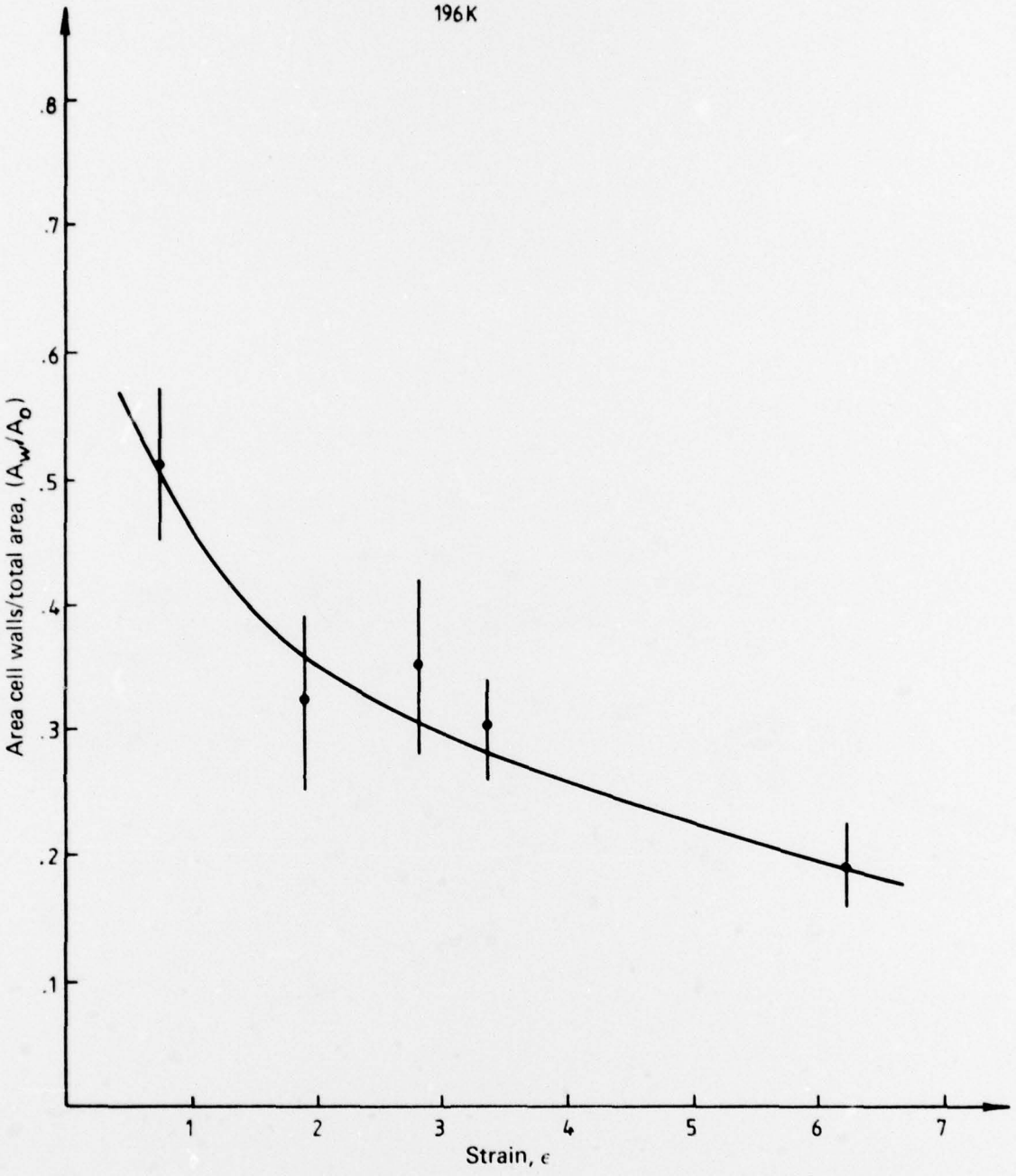

Fig. 12 The ratio of dislocation wall area (A_w) to total cross sectional area (A_o) of copper wires as a function of total drawing strain (ϵ).

(a) Temperature of drawing 196K

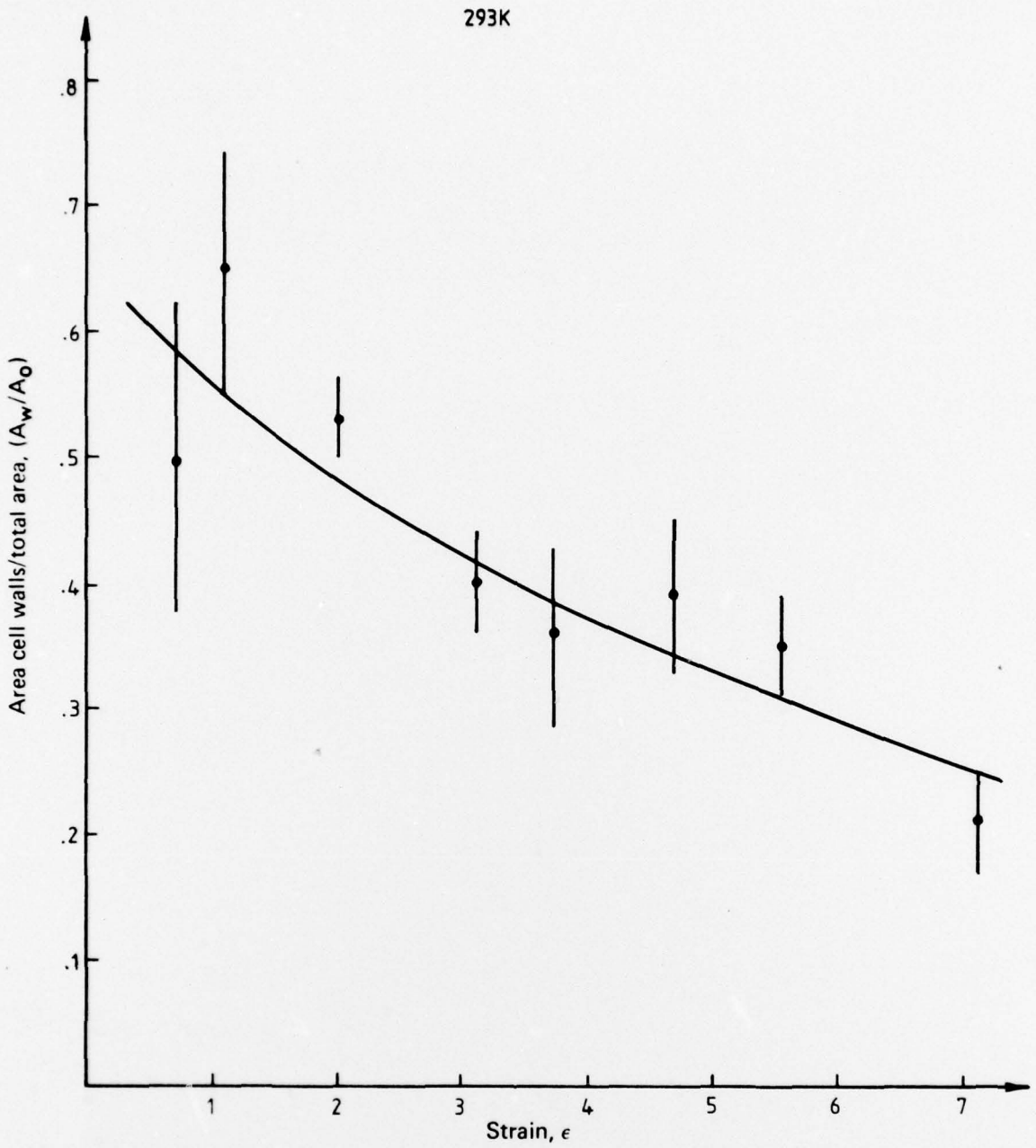

Fig. 12 cont.

(b) Temperature of drawing 293K

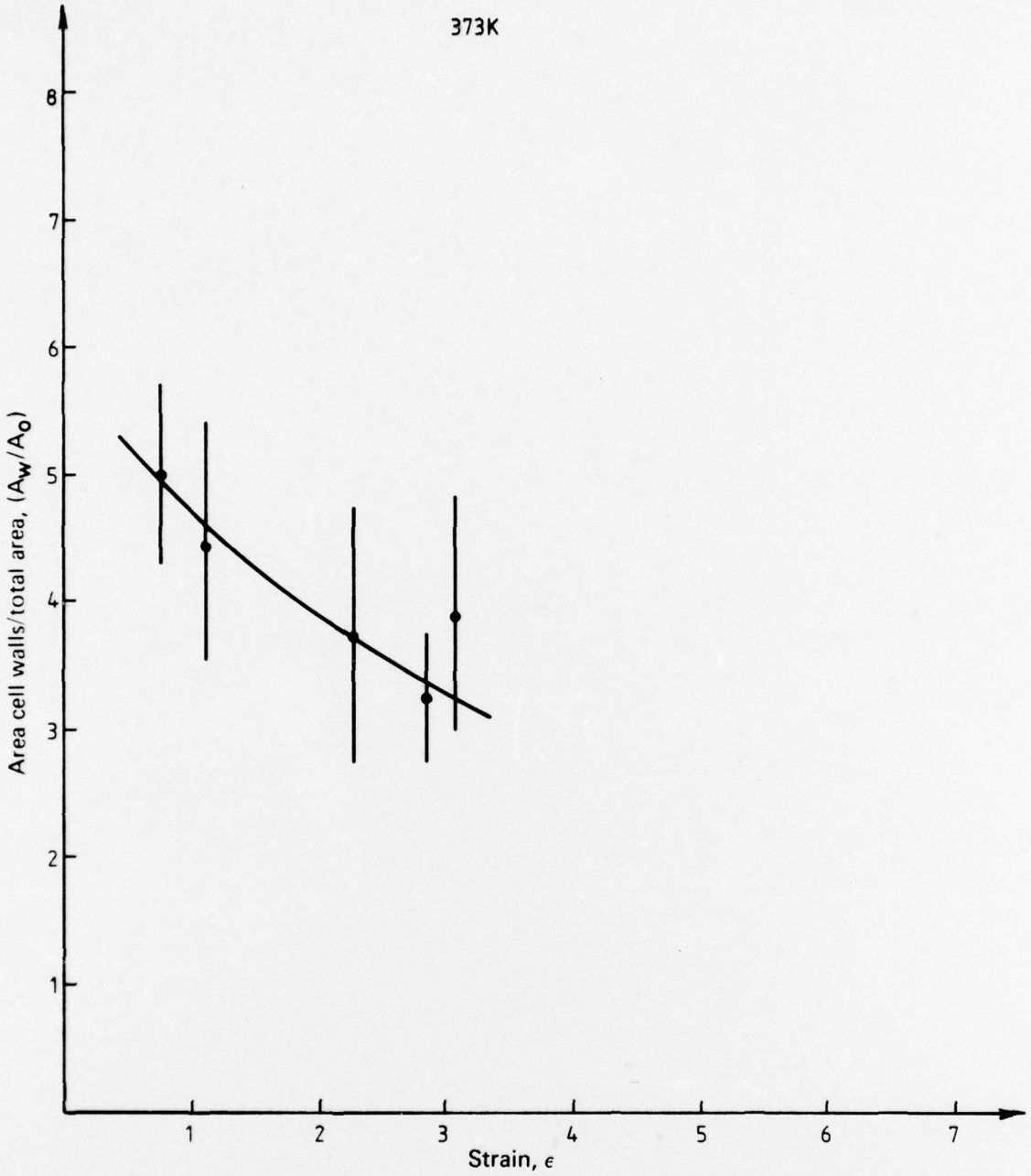

Fig. 12 cont.

(c) Temperature of drawing 373K.

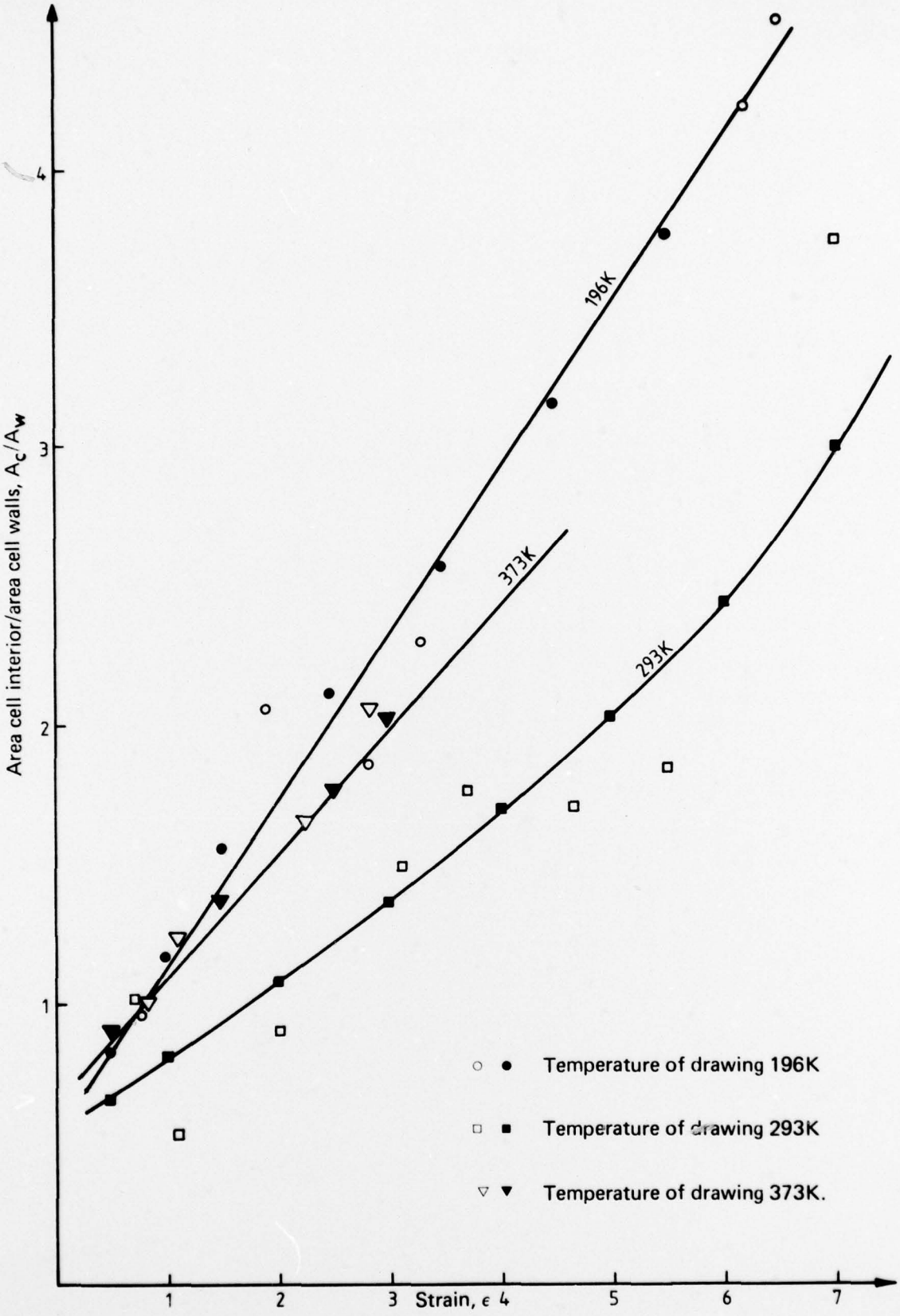

Fig. 13 The ratio of area of dislocation-free-regions (A_c) to dislocation wall area (A_w) as a function of total drawing strain (ϵ) for three temperatures of drawing.

Fully shaded points: A_c/A_w obtained using smoothed curves of Figure 12.

Unshaded points: A_c/A_w obtained using experimental results shown in Figure 12.

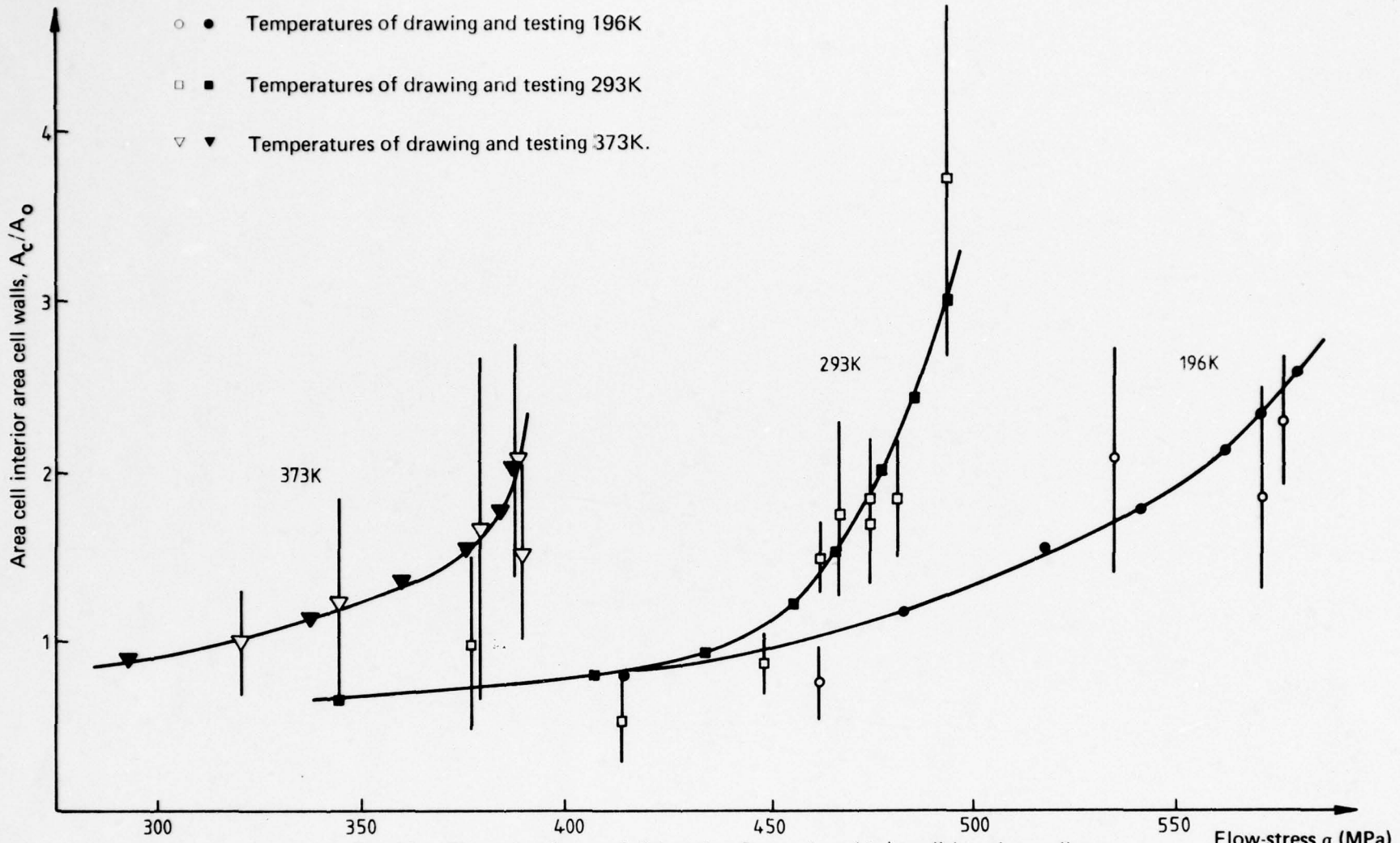

Fig. 14 The ratio of area of dislocation free regions (A_c) to dislocation wall area (A_w) as a function of flow stress (σ) for three temperatures of drawing.
Fully shaded points: A_c/A_w and σ obtained from smoothed curves of Figures 9 and 13.
Unshaded points: A_c/A_w and σ obtained from experimental results of Figures 9 and 13.

REFERENCES

1. Holt, D. L. — J. Appl. Phys., *41*, 3197, (1970).
2. Hall, E. O. — Proc. Phys. Soc. London, *B64*, 747, (1951).
3. Petch, N. J. — J. Iron and Steel Inst., *174*, 25, (1953).
4. Kalish D., and Le Fevre, B. G. — Met. Trans., *6A*, 1319, (1975).
5. Wingrove, A. L. — J. Inst. Metals, *100*, 313, (1972).
6. Embury, J. D., Keh, A. S., and Fisher, R. M. — Trans. Met. Soc. A.I.M.E., *236*, 1252, (1966).
7. Warrington, D. — Proc. European Conference on Electron Microscopy, 1960, Delft. Ed. Houwink and Spit.
8. Langford, G., and Cohen, M. — Met. Trans., *1*, 1478, (1970).
9. Hutchison, M. M., and Pascoe, R. T. — A.R.L. Report, Met. 85, September 1971.
10. Fujita, H., and Tabata, T. — Acta Met., *21*, 355, (1973).
11. Bailey, J. E. — Phil. Mag., *8*, 223, (1963).
12. Bailey, J. E., and Hirsch, P. B. — Phil. Mag., *5*, 485, (1960).
13. Li, J. C. M. — J. Appl. Phys., *33*, 2958, (1962).
14. Bullen, F. P., and Rogers, C. B. — Phil. Mag., *9*, 401, (1964).
15. Hutchison, M. M., and Pascoe, R. T. — J. Aust. Inst. Metals, *14*, 308, (1969).
16. Langford, G., and Cohen, M. — Met. Trans., *6A*, 901, (1975).
17. Cairns, J. H., Clough, J., Dewey, M. A. P., and Nutting, J. — J. Inst. Metals, *99*, 93, (1971).
18. Li, J. C. M. — Recrystallization Grain Growth and Textures, A.S.M. 1966.
19. Cahn, R. W. — Recrystallization Grain Growth and Textures, A.S.M. 1966.
20. Hu, H. — Recovery and Recrystallization of Metals, Ed. Himmel, Interscience 1963.
21. Luton, M. J., and Sellars, C. M. — Acta Met., *17*, 1033, (1969).
22. McQueen, H., Wong, W. A., and Jonas, J. J. — Acta Met., *15*, 586, (1967).
23. Hardwick, D., and Tegart, W. J. McG. — J. Inst. Metals, *90*, 17, (1961-62).
24. McQueen, H., and Bergerson, S. — Metal Science Journal, *6*, 25, (1972).
25. Ray, R. K., Hutchinson, W. B., Besag, F. M. C., and Smallman, R. E. — Journal of Microscopy, *97*, 217, (1973).

26.	Tegart, W. J. McG.	Ductility, A.S.M. 1967.
27.	Clarebrough, L. M., Loretto, M. H., and Hargreaves, M. E.	Recovery and Recrystallization of Metals, A.I.M.E. 1963.
28.	Nethercott, R. B., and Coyle, R. A.	A.R.L. Report, Mat. *99*, 1975.
29.	Hutchinson, W. B.	Metal Science, *8*, 185, (1974).
30.	Okada, A., Mitsuji, H., and Nakae, H.	Trans. Japan Inst. Metals, *15*, 417, (1974).
31.	Nethercott, R. B.	A.R.L. Report, to be published.
32.	Van Buren, H. G.	Imperfections In Crystals, North Holland 1960.
33.	Nethercott, R. B.	Proceedings I.I.W. 1976 and Metals Technology Conference. Sydney 1976, page 8-10-1.

DISTRIBUTION

Copy No.

AUSTRALIA

DEPARTMENT OF DEFENCE

Central Office

Chief Defence Scientist	1
Executive Controller, A.D.S.S.	2
Superintendent, Defence Science Administration	3
Defence Library	4
J.I.O.	5
Assistant Secretary, D.I.S.B.	6–21

Aeronautical Research Laboratories

Chief Superintendent	22
Superintendent, Materials Division	23
Divisional File, Materials Division	24
Authors: R. B. Nethercott	25
J. A. Retchford	26
Library	27

Materials Research Laboratories

Library	28

Weapons Research Establishment

Library	29

STATUTORY, STATE AUTHORITIES AND INDUSTRY

Australian Atomic Energy Commission (Director) N.S.W.	30
CSIRO Central Library	31
CSIRO National Measurement Laboratory (Chief)	32
CSIRO Tribophysics Division (Director)	33
Western Australian Government Chemical Laboratories, Library	34
B.H.P. Central Research Laboratories, N.S.W.	35
B.H.P. Melbourne Research Laboratories	36
Comalco Research Laboratories, Victoria (Dr. J. Eady)	37
Conzinc Riotinto of Australia, Victoria (Dr. Worner)	38

UNIVERSITIES AND COLLEGES

Adelaide	Barr Smith Library	39
Australian National	Library	40
Flinders	Library	41
James Cook	Library	42
La Trobe	Library	43
Melbourne	Engineering Library	44
Monash	Library	45
	Professor I. J. Polmear	46
Newcastle	Library	47

UNIVERSITIES AND COLLEGES

Birmingham	Dept. of Physical Metallurgy and Science of Materials (Prof. R. E. Smallman)	85
	Dept. of Physical Metallurgy and Science of Materials (Dr. W. B. Hutchinson)	86
Bristol	Library	87
Cambridge	Library, Engineering Dept.	88
	Professor R. W. K. Honeycombe, Dept. of Metallurgy	89
Leeds	Professor J. Nutting, Dept. of Metallurgy	90
Newcastle	Dr. J. T. Evans, Dept. of Metallurgy	91
Nottingham	Library	92
Oxford	Dr. T. Hazzledine, Dept. of Metallurgy	93
Sheffield	Dr. C. M. Sellars, Dept. of Metallurgy	94
Southampton	Library	95
Strathclyde	Library	96
Sussex	Professor R. W. Cahn, School of Engineering and Applied Science	97
Cranfield Institute of Technology	Library	98
Imperial College	The Head	99

UNITED STATES OF AMERICA

Counsellor Defence Science		100

UNIVERSITIES AND COLLEGES

Georgia Institute of Technology	Professor B. G. LeFevre, Metallurgy Dept.	101

Spares 102–112